Impact Modelling of Zirconia Toughened Alumina and Kevlar Hybrid Composite

Author

Talha Imran

Regn Number

NUST2018SMME-0000276032

Supervisor

Dr. Samiur Rahman Shaha

DEPARTMENT SMME

SCHOOL OF MECHANICAL & MANUFACTURING ENGINEERING

NATIONAL UNIVERSITY OF SCIENCES AND TECHNOLOGY

ISLAMABAD

JULY 2021

Impact Modelling of Zirconia Toughened Alumina and Kevlar Hybrid Composite

Author

Talha Imran

Regn Number

NUST2018SMME-0000276032

A thesis submitted in partial fulfillment of the requirements for the degree of

MS Mechanical Engineering

Thesis Supervisor:

Dr. Samiur Rahman Shah

Thesis Supervisor's Signature: _____

DEPARTMENT SMME

SCHOOL OF MECHANICAL & MANUFACTURING ENGINEERING

NATIONAL UNIVERSITY OF SCIENCES AND TECHNOLOGY,

ISLAMABAD

JULY 2021

Declaration

I certify that this research work titled *'Impact Modelling of Zirconia Toughened Alumina and Kevlar Hybrid Composite"* is my own work. The work has not been presented elsewhere for assessment. The material that has been used from other sources it has been properly acknowledged /referred.

Signature of Student

Talha Imran

NUST2018SMME-0000276032

Plagiarism Certificate (Turnitin Report)

This thesis has been checked for Plagiarism. Turnitin report endorsed by Supervisor is attached.

Signature of Student

Talha Imran

NUST2018SMME-0000276032

Signature of Supervisor

Dr. Samiur Rahman Shah

Copyright Statement

Acknowledgements

I am thankful to my Creator Allah Subhana-Watala to have guided me throughout this work at every step and for every new thought which you setup in my mind to improve it. Indeed, I could have done nothing without your priceless help and guidance. Whosoever helped me throughout the course of my thesis, whether my parents or any other individual was your will, so indeed none be worthy of praise but you.

I am profusely thankful to my beloved parents who raised me when I was not capable of walking and continued to support me throughout in every department of my life.

I would also like to express special thanks to my supervisor **Dr. Samiur Rahman Shah and Dr. Owaisur Rahman Shah** for their help throughout my thesis. I can safely say that I have not learned any other engineering subject in such depth than the ones which they have taught.

Finally, I would like to express my gratitude to all the individuals who have rendered valuable assistance to my study.

Dedicated to my exceptional parents and adored siblings whose tremendous support and cooperation led me to this wonderful accomplishment.

Abstract

Engineering structures like those with applications in aerospace industry, marine industry and sports industry etc. have composite materials under impact loads. Understanding of failure characteristics of composite materials under various loading condition is essential to ensure a reliable design and to avoid catastrophic failure. The damage behaviour of composites has been under research for different loading conditions. Most of the research studies have focused the failure under quasi-static loading and low velocity impact loading. However, damage behaviour under high-energy impact is a completely different phenomenon than the former. In addition, very few studies are available on the damage modelling of fibre-ceramic sandwich structures. This thesis is an attempt to further extend the understanding of failure of composite materials by investigating the damage behaviour under high-energy impact loading.

The research methodology adopted utilizes an analytical modelling and numerical simulations of composite materials under impact loading. The analytical model is derived using laminate theory and fracture mechanics as a strength based and energy-based approach respectively. Finite element analysis (Explicit dynamic) is carried out using a commercially available software ABAQUS 6.13. Simulation model is benchmarked with published literature and showed good correlation.

It is observed that energy absorption increases with increase in interface area by changing the tile configuration of core for a range of impact energy (0-40J). While, solid core shows dominant energy absorbing behaviour at high-energy impacts (>40J). However, placing the ceramic core results in increased damage energy value throughout as compared to pure composite panel.

Moreover, as the impact energy increases the material behaviour tend to be more brittle in nature and delamination at the interface of tiles in ceramic core is no longer a dominant failure mode, which is the result of high rate of loading. In addition, the core shatters as soon as the projectile hits the panel and tensile failure of fibre is now predominant.

Table of Contents

List of Figures

List of Tables

Chapter 1

1. Introduction

Fibre-reinforced composite materials, due to their supremacies like high stiffness, high strength, low density along with design flexibility, have progressively replaced the conventional metallic materials and are very widely used in many engineering fields including aircrafts, satellites and their use has extended especially in aerospace, military and automotive industries. Despite the vast applications, composite material suffer due to their low damage resistance under impact loads and the problem becomes more critical when used in extreme environments. Impact damages substantially lowers the load carrying capability of composite structure, which ultimately leads the way to its failure. Hence, the study of damage modelling of fibre based composite materials under impact loads is of paramount importance. Damage modes differ greatly when subjected to various levels of impact energy as rigorous perforation happen under high-energy impacts. While low energy impacts results in the development of different modes of failure such as delamination, fibre fracture and matrix failure. Experimentally, it is very strenuous to analyse all these modes of failure because they remain concealed in between plies. It is even harder to trace their progression during experiments. Therefore, a finite element method (FEM) is an efficient way to study these significantly important complexities, as FEM will greatly reduce the complexities and limitations in analysis. Moreover, energy absorption capacity of composites suffers significantly under impact loads. Introduction of metallic or ceramic sandwich cores in between laminates can improve this aspect. In order to utilize this strategy to our advantage, the detailed investigation of its effect on energy absorption and stiffness improvement is very important.

1.1 Overview

Structural applications of fibre reinforced composite materials are progressively growing in different industries e.g. aerospace, aeronautics etc. However, composite material applications are limited even today because of difficulty in their service life prediction and still commercial aircraft use many components mainly composed of metallic materials. Use of composite material will spread further along with the understanding of material behaviour and damage. Therefore, to study the damage behaviour of composite material in different loading condition is of paramount

importance before them being used in a specific application. Hence, it is necessary to understand the different type of failure occurring in composite materials.

1.2 Zirconia Toughened Alumina

ZTA Tiles with Rubber (Zircon Toughened Alumina) from HMA Wear Solutions includes a metal plate that makes the metal. These are suitable for high impact use, as the rubber absorbs energy, thus preventing tiles from breaking. The panels are easy to replace due to studs mounted on a support plate. The biggest advantage of Zirconia Toughened Alumina (ZTA) from HMA Wear Solutions is more strength and durability than Alumina, combined with lower cost. The combination of aluminium oxide and zirconium oxide provides much stronger strength, durability, durability, and wear resistance than Alumina alone. A 20% to 30% increase in strength often provides the design requirements required at a much lower cost than using only zirconia alone. [1]

Alumina-based ceramics are successfully used as cutting, mortar or synthetic tools. Failure under those service-related conditions is often associated with the low to moderate hardness value shown by alumina ceramics. The development of zirconia-toughened-alumina (ZTA) compounds is intended to incorporate alumina ceramics into applications where high resistance is required. Zircon Toughened Alumina materials contain an alumina matrix in which there are embedded, unstable or stable zirconia particles. Such a second phase increase leads to an increase in flexural strength, stiffness and fatigue resistance, mainly due to the reversal of the phase caused by stress that tetragonal zirconia enters a strong monoclinic phase. This phase shift is accompanied by an increase in volume (~4%) which creates pressure pressures around the diffuse split and enhances the attractive effect. Therefore, the volumetric fraction of additional zirconia was found to be directly related to resistance to Zircon Toughened Alumina compounds. On the other hand, it has also been observed that microstructure stiffness within Zircon Toughened Alumina may result in an increase in stiffness. Such a combination is associated with an important effect of zirconia particle size on phase transformation and the influence of large matrix particles on the promotion of grain brittleness and deformation cracking. Therefore, the study of the emergence of the microstructure of Zircon Toughened Alumina, depending on the size of the matrix particles and the particle size of the zirconia, and its effect on the strength of the fragmentation appears to be very interesting studies. Fluid solution and sodium silicate, such as nucleating agent; they were

used to increase bone-like apatite layer in the composite substrate of ZTA by biomimetic process. Use of sodium silicate solution instead of bioactive glass encouraged the incorporation of compacted carbonated hydroxyapatite layer into the ZTA substrate a bone-like apatite layer in the composite Zircon Toughened Alumina substrate, moderate body fluid and sodium silicate solution were used as nucleating agent. It was found that sodium consumption. Silicate solution improves the placement of the composite layer of carbonated hydroxyapatite in the ZTA substrate. In an effort to improve machine power and incompatibility of ZrO2-Al2O3-HA, Nano-composite powder pressurized to a temperature of 1400 ° C. composed of biphasic calcium phosphates (BCP) [HA / TCP] and ZrO2-Al2O3. Increasing HA content is improving the increase and variability of the behaviour of cells like osteoblast in composite.[2]

Alumina, zirconia, and zirconia alumina alloy (ZTA) are among the pottery materials considered hip roots. This is especially true of alumina, which has been proven to be the most effective foundation for complete hip transplants to date. Alumina has a variety of benefits, including high biocompatibility integration, mechanical strength, and resistance to cracking. However, ceramic can have disadvantages, such as the body's response to implants. In addition, wearing debris in contact areas can cause bone regeneration, which has led to an inflammatory response and implant implantation. The main issues which are limiting the lifetime of present implants are aseptic loosening and bone resorption. Alumina-containing ceramics comes in many hygienic standards, and their mechanical properties are controlled by this purity. The particle size of the alumina ranges from a few to tens of microns, and the high purity of alumina ceramics is used in biological applications.[3]

Zirconia, like alumina, has excellent material properties. Zirconia has many benefits, including low corrosion levels, chemical stability, and mechanical strength. In addition, the new zirconia module is equivalent to that of stainless-steel alloys. Because of this, this ceramic is thought to have great biomaterial strength.

Hip implants use zirconia toughened alumina which is very promising material. ZTA has many advantages, including high mechanical properties of yttria stabilized zirconia and high inertness of alumina, but none of its disadvantages, as well as high wear resistance, high cracking resistance, and high chemical strength of advanced durability. ZTA is produced with various amounts of

zirconia particles, and its mechanical properties change as the amount of zirconia changes. Zirconia particles are mixed with alumina particles, covering some of the gaps between them. This increases durability because the voids in the ceramic will reduce strength and increase the risk of cracking. Mechanical properties of zirconia, ZTA and alumina have been shown in table below.

Table 1-1 Mechanical properties of ceramics biomaterials [1]

	Modulus of elasticity (MPa)	**Poisson ratio**
Alumina	374 000	0.21-0.23
Zirconia (monoclinic) (Eichler et al., 2004)	92 000 ~ 244 000	0.22
Zirconia toughened alumina	360 000	0.23

1.3 Research Problem

The purpose of this research is to study and characterize Kevlar based composite material. In this regard a numerical model is developed for analysing the progression of different damage modes of fibre based composite material under varying impact energies. Further, this study aims to investigate the effect of placing a ceramic sandwich core in between plies on energy absorption and failure modes under impact loads.

1.4 Research Objectives

The aim of this study is the failure analysis of composite materials subjected to impacts with external objects. Different damage modes will be investigated under varying levels of impact energies. The effect of placing a sandwich core on the absorbed energy and evolution of failure modes will be studied as well. The study is accomplished by the following proposed objectives:

- To develop an analytical model for the analysis of absorbed energy
- To perform tensile testing on composite material
- To perform Peel test on sample material to get G_{IC} for FEA

- To perform design calculations for the determination of sandwich core thickness and dimensions of different cell shapes.
- To develop a CAD model for Finite Element Analysis (FEA)
- To develop numerical model for simulations of all the described scenarios.
- To compare and validate the numerical model with published literature.
- To perform simulations of our model under the described loading condition and other scenarios.
- To analyse and discuss the results obtained.

1.5 Outlines

To discuss important aspects of the present study, this thesis is structured into seven chapters delineated below. The outline of thesis provides brief details of the work presented with in each chapter.

Chapter 1 (Introduction) contains the motivation behind this study and problem statement. Aim and objectives of the proposed study are precisely outlined to provide an overview of the project goals. Different methods and techniques that have been used in different section are also mentioned.

Chapter 2 (Literature Review) encompasses the broad literature review of research work relevant to this study.

Chapter 3 (Mathematical Modelling) comprises of an empirical model that describes the effect of strain rate on constitutive properties of composite materials. The relations are developed using linear regression technique implied on the experimental data available. It also includes the analytical model for the failure analysis of composite material along with the calculations of damage energy dissipation.

Chapter 4 (Model Design and Numerical Modelling) covers the detailed description of our Finite Element Model. CAD model, material behaviour models, damage models, mesh convergence, model validation and solution convergence are specified in detail in this chapter.

Chapter 5 (Results and Discussion) contains results of impact simulations performed under different impact energies. Details of evolution of different damage modes and energy absorption are also discussed.

Chapter 6 (Conclusion, Recommendations and Future Work) presents the concluding remarks with some recommendations followed by future work.

Chapter 2

2. Literature Review

Fibre-reinforced composite materials have been widely used in many engineering fields including aircrafts, satellites, boats etc. They are especially being used in aerospace, military and automotive industries due to their high strength, high stiffness, low density and designability. In addition, they have good fatigue performance and corrosion resistance. In view of all these qualities, an expansion happened in the use of composite in extreme environment. Therefore, it is very essential to study the mechanical behaviour of composite materials and their corresponding damage modes under various loading scenarios. Impact event happens to be one such critical loading condition, which is a sophisticated phenomenon as it includes a very intricate stress distribution in the material, e. g. compression at the top, tension at the bottom, interlaminar shear stress inside the laminate and contact stress just behind the projectile. Hence, behaviour of composite materials under high strain rate loading gained much attention in last few years. Anisotropic and inhomogeneous nature of composites made the analysis of damage modes and failure complex and difficult to investigate. Therefore, wide varieties of experimental, numerical and analytical studies were carried out to analyse the dynamic response of fibre-based composite materials under high strain rate loading.[4]

2.1 Historical Background

Composite materials studies were started in 19th century and various solutions were presented by different researchers. Initially, composite materials were analysed under simple static loading condition such as tensile, compressive and bending loading proceeded by studies under dynamic loading conditions. Later, failure investigation in composite material became main focus. In this regard, major breakthrough is provided by Tsai-Hill. Their work is based on maximum stress strategy along principal direction. Tsai-Wu then added another term to focus more on shear behaviour [8], [9]. Hashin and Hill considered shear behaviour in both longitudinal and transverse modes and treated matrix and fibre damage modes separately. Further improvement came from Puck especially in matrix compression failure mode.[5]

2.2 Longitudinal Tensile Behaviour

Prior to the development of constitutive models, various experiments were conducted on composite materials. As composite materials are anisotropic in nature, uniaxial loads were applied along different direction were applied on composite materials. Unidirectional longitudinal tension tests of carbon fibre composite materials were conducted by Ishikawa et al [10]. They observed that longitudinal modulus increases with strain or stress unto an intermediate level. Zhou et al carried out dynamic longitudinal tensile testing of carbon fibre based composite materials using bar-bar tensile impact apparatus (BTIA). It was concluded that tensile strength and strain to failure increases with strain rate due to strain rate strengthening effect. However, longitudinal modulus of carbon fibre is seen to be independent of strain rate [8].

2.3 Longitudinal Compressive Behaviour

In comparison to tensile behaviour, evaluation of longitudinal compressive strength of composite materials is very difficult because of fibre buckling under compression. New methods with certain variations were proposed for the investigation of longitudinal compression behaviour of fibre-based composite materials. In the study performed by Kyriakides et al, compression tests were performed on cylindrical rods and thin walled ring specimens. Results indicated that fibre imperfections introduced during curing of laminate and manufacturing of the prepreg of the composite play a crucial role in deciding the actual strength of fibre-based composites. [6] Failure in such cases happens due to bending stresses in the form of kinking of fibres along planes with non-zero inclination to the transverse direction of composites. Bing and Sun proposed a new technique for testing of fibre-reinforced composites in compression. They established that the covering of titanium coating at the specimen ends can significantly lower the contact friction and hence consistent stresses can be achieved, thus allowing the shear-extension coupling to develop fully. Experiments conducted by Hsiao et al showed that initial modulus increases slightly with strain rate, whereas ultimate strain and the strength under dynamic loading are significantly greater than the quasi-static values. Both longitudinal and transverse compression tests results indicated the similar trends.[7]

2.4 Transverse Tensile and Compressive Behaviour

In the second principal direction perpendicular to longitudinal direction of fibre, the mechanical behaviour was dominated by the matrix and fibre-matrix interface properties. Study of dynamic inter-fibre failure of UD composite laminates was carried out by Cui et al indicated that through thickness reinforcement showed very little influence on inter-fibre strength in compression. While, the strength is reduced significantly in tensile and shear failure modes at elevated strain rates as compared to quasi-static loading conditions. Tun et al used the concepts of plasticity with damage to investigate the composite failure in transverse direction [6]. No progressive failure was observed, rather the material showed a nonlinear response in both transverse and shear directions due to non-linear nature of matrix material. Hence, composite material always showed the nonlinear behaviour in transverse direction because of the nonlinear nature of matrix material. Ghazi et al proposed a micromechanical damage model based on volumetric crack-density (VCD) to investigate the influence of matrix cracking on constitutive behaviour of composite materials. The model concluded that matrix cracking in loaded laminate, is the major cause of intimate non-linear behaviour of composite materials. Koyanagi et al investigated the transverse tensile behaviour of unidirectional (UD) fibre-reinforced composite materials [4]. Cohesive zone modelling was employed for fibre-matrix interface to consider mixed-mode interfacial failure.[8] Simulations showed that the interface failure is prominent at high strain rate, while matrix failure usually occurs at low strain rates due to barely visible impact damages (BVID). Li et al studies the effect of the irregular pores on transverse behaviour of carbon fibre-based pyro carbon composites. Experiments conducted by Hsiao et al using a drop weight method and split pressure Hopkinson bar technique for dynamic characterization showed that initial modulus increases slightly with strain rate, whereas ultimate strain and the strength under dynamic loading are significantly greater than the quasi-static values. Both longitudinal and transverse compression tests results indicated the similar trends and showed that transverse compressive strength increases rapidly with strain rate.[9]

2.5 In-plane and Out-of-plane Shear Behaviour

Besides, study of shear behaviour of composite laminae under strain rate loading is of remarkable importance. Johnson et al. presented a Continuum Damage Mechanics (CDM) model to investigate

the in-plane response of fabric-reinforced composites. The model is useful in predicting failure modes but delamination damage is neglected. A finite element analysis was performed by Johnson et al. to model the in-plane failure in fabric-reinforced composites. The effect of delamination on strength reduction is also considered. McCarthy et al. performed an experimental study to characterize the constitutive behaviour of composites under shear loading. Cubic spline interpolation method was implied to develop a 3-dimensional damage model, able to describe nonlinear shear behaviour and predict large shear strains with good accuracy.[10] An experimental and numerical study of in-plane shear behaviour of fibre-reinforced composites was performed by Totry et al. For strain measurement, digital image correlation (DIC) and strain gauges were used. Results indicated that in-plane shear response of composites consists of three regimes [7]. A linear elastic region totally dependent on elastic properties and volume fraction of matrix and fibre, followed by a nonlinear region which began with the onset of matrix plastic deformation and end with a hardening region affected by fibre rotation and interface fracture. Experiments were conducted by Papadakis et al. on twenty-two [±45] 2s laid up specimens of glass-fibre-reinforced thermoplastic (GFRP) composites laminates for the investigation of shear behaviour over various strain rates. Results depicted that shear strength is in direct relation with strain rate, while shear modulus decreased with increasing strain rate. Besides, failure strain is seen to be insensitive to strain rate [11]. Eskandari et al developed a constitutive model to study the visco-plastic effects on damage of composite materials. They observed that the model is suitable to accurately predict damage onset under medium and low strain rate loading and in-plane shear is predominantly the damage mode. Hence, it was concluded that shear damage progression is highly dependent on strain rate [10]. Marin proposed a promising way to further investigate the shear behaviour by means of a simple off-axis tensile test using oblique end tabs whose inclination coincides with that of the longitudinal isodisplacement lines. Hajikazemi et al. developed a variational model to determine the variation in shear laminate properties and stress transfer mechanism. It was revealed that the presence ply cracks significantly reduce out-of-plane shear stiffness caused by perturbed uniform stress distribution. Hence, it was concluded that shear damage evolution is highly strain rate dependent [9].

Studies that have been reported in literature, these are mainly focused on behaviour of material under static, quasi-static and under low strain rate loading. There is a lack of study on damage

behaviour of composite materials under high strain rate loading. Apart from that damage onset and damage progression under dynamic loading need to be investigated in depth to distinctly reveal the failure mechanism of fibre reinforced composite materials [8].

2.6 Failure Criteria

Based on the experimental data, constitutive relations were developed to model the behaviour of composite material. Besides, to estimate the strength of fibre and matrix, other studies were performed to focus on failure criteria. Hashin established the failure criteria based on the transversely isotropic stress invariants. Four distinct failure modes for composites are: tensile and compressive failure modes for both fibre and matrix. Failure criteria proposed by Puck includes both fibre failure and inter fibre fracture. Tsai and Wu developed a strength-based failure criterion for anisotropic composite materials which mainly focuses on the fracture surface as an improvement from other criteria. Tuo et al. investigated the behaviour of composite laminated under low velocity impact and compression after impact (CAI) loads both experimentally and numerically. Three-dimensional Puck criterion and maximum strain failure criterion were implied to analyse initiation of matrix and fibre damage and damage evolution was captured by using bi linear damage constitutive relation. They concluded that the delamination area increases with increase in impact energy and multiple impacts, and local buckling initiates from the impacted region and moves towards outer boundary during CAI load. Richardson and Wisheart presented a review of low velocity impact properties of composite materials [11]. They described the modes of failure under low velocity impacts and the conditions during which a particular damage mode is most vulnerable. Hou et al. studied the implementation of failure criteria to carry out prediction of impact-induced damage in composite plates. The effect of out of plane stresses for damage initiation and interaction between different damage modes were also incorporated in the model. For the first time, they suggested that delamination is constrained by through thickness compression stresses. It was observed that compression stresses in thickness direction helps in suppressing delamination. Hou et al. further extended their study for improvement of delamination failure criterion for composite laminate structures under low velocity impact (LVI) load. They also considered the effect of high local interlaminar shear stresses induced by matrix cracking and fibre failure on delamination which resulted in reduced interlaminar shear strength. Li et al. performed finite element analysis (FEA) to assess different failure criteria and damage evolution methods for

analyzing the behaviour of composite laminates under LVI loading condition. To encapsulate the interface delamination cohesive elements are used in between adjacent laminates. It is observed that maximum stress-based criteria show large deviation in predicting damage shape, area and propagation in most of the failure modes as compared with experimental data. While energy dissipation and equivalent strain based criteria showed good correlation with experimental data [12].

2.7 Damage Progression

In parallel, some other studies were carried out focusing on degradation process of composite materials before the final failure. Some parameters that need to be considered during damage progression of composite material are: viscosity, damage and plasticity. Yield criterion presented by Hill was generally used for the consideration of plasticity in damage behaviour and superposition method was employed to include the effect of viscosity. Ladeveze and Dantec studied the effect of matrix microcracking and delamination damage on mechanical and rupture properties of laminated composites. For this purpose, used continuum damage mechanics approach and observed that ply degradation is directly linked with rupture behaviour of laminated composites. Nakatani et al. performed a study on the impact-induced damages to investigate the extent of internal damage in the in-plane direction. They also studied the effect of energy absorption on matrix microcracks and residual out of plane deformation by placing a core in between laminates. The study revealed that the placement of a metal layer on the side opposite to impact results in suppressing the internal and out of plane damages as energy is absorbed in plastic deformation of the layer. Study on the delamination damage behaviour of thick composite laminates subjected to low-energy impact is carried out by Wang et al for different stacking sequences and under different energy levels[13]. They discussed that the delamination length close to the impact face is a larger value than near the bottom face with increase in impact energy. Freitas et al. worked on the failure mechanisms and damage growth of composite specimens subjected to impact loading. They also studied the effect of stacking sequence and thickness of panel on damage mechanism and concluded that delamination area is greatly affected by impact energy but is also dependent of stacking sequence. Interaction between interlaminar and intralaminar damage mechanism is investigated by Bruno et al. Their damage mechanisms included a general approach based on both Continuous Damage Mechanics and Fracture Mechanics to predict coupled

distributed in plane damage effects and interlaminar crack growth. It is concluded that values of ERR predicted by LEFM are higher than predicted by CDM as intensification of ERR happens due to interaction between interlaminar and intralaminar damage mechanisms and that consequently overestimates the load carrying capacity [14]. The same effect is studied by Yun et al. to predict the failure behaviour and the ultimate load bearing capacity of fibre reinforced polymer (FRP) laminates. A cohesive zone method with mixed bilinear law is used for delamination modelling and material property degradation method for intralaminar cracking. The model investigates the progressive damage failure and coupling effect of multiple failure modes. A study of time and temperature dependent damage behaviour of particulate composite is carried out by Park. The developed model includes the effect of changing microstructure and damage progression on mechanical behaviour of material. Iannucci used thermodynamic maximum energy dissipation approach for progressive failure modelling of thin woven carbon composites under impact load. The approach entails controlling damage evolution and thus energy dissipation rather than damage. The maximum energy dissipation approach proved to be more useful for accurate determination of damage growth rate and prediction of correct damage pattern as compared to stress-based approach. Schuecker worked on the development of a damage model to describe the deterioration of material properties as a result of damage evolution. Concentration on matrix influenced damage modes, damage conduct is part into two contributions: damage progression in consequence to load and effect of damage as a function of damage modes and stress state. Mechanical behaviour of UD fibre-reinforced laminated composites is modelled by Liang. It was indicated that fibre/matrix debonding and seeding of cracks resulted in gradual loss of strength [15].

2.8 Progressive Damage Modelling Under High Strain-rate Loading

Chen and Morozov carried out the development and validation of a consistency elasto-viscoplastic damage model for composite materials. It is observed that model is well suited for progressive failure analysis of composite materials subjected to loadings at various strain rates. An experimental and numerical investigation was performed by Khan et al. to observe the damage mechanism and delamination pattern under low energy impact load (LVI) with different energy levels. Cohesive zone method and Hashin failure criterion are used to study interlaminar and intralaminar damage behaviour. It is observed that matrix cracking occurs first followed by the

delamination and the delamination area increases which is dominated by increase in length rather than width with increase in impact energy. Medikonda and Tabiei investigated the delamination in composite laminates numerically [16]. They also incorporated the strain rate dependence effect. Through-thickness stretch elements were used to study the effect out of plane stresses on delamination. Results showed that the effect of out of plane stresses in overall delamination prediction is small but it cannot be ignored especially in impact simulations. Khan and Sharma further extended their previous study for prediction of damage progression in composite laminates exposed to low velocity impact load. Interface delamination was also considered in this study. It is observed that delamination dissipation energy is highest. But for higher impact energy levels, energy dissipation due to fibre failure increases. They also investigated the metal layer placement effect on the damage and energy absorption mechanism in aluminum/glass fibre laminates both numerically and experimentally under low velocity impact (LVI) loads. Finite element analysis was performed with the help of user subroutine model in ABAQUS VUMAT to consider Hashin failure for predicting the response of composite layer. It is concluded that placement of metal layer lowers the impact damage resistance, but the absorbed energy is increased with decrease in delamination. An energy-based approach has been by used by Iannucci and Ankersen for damage modelling of thin woven and unidirectional (UD) composite materials. The model is useful for investigation of strain rate dependent behaviour of composite materials. It is observed that matrix dominated damage modes such as shear response show high strain rate dependence which is similar to the results of before mentioned studies. The damage behaviour of thick laminated composite materials is studied using a Continuum Damage Mechanics (CDM) model by Randles and Nemes. Maximum strain criterion is used for fibre damage. The model is capable of representing non-linear rate dependent behaviour. Aktay et al. performed a numerical analysis for investigating the damage behaviour of composite sandwich panels under high velocity transverse impact loads. They numerical model provides good details of HV impact on sandwich structures including force, displacement, velocity and energy response and damage development during impact. A numerical model for damage under high strain rate load based on fracture energy-based damage mechanics approach is developed by Iannucci and Willows. They concluded that in plane shear failure mode is observed at typically large strains with high rate dependency [17].

It is concluded from the detailed study of literature that work has been done on failure of composite under both static and dynamic loading of different nature. Behaviour of composite material under low velocity impact loads has been investigated in sufficient detail. Therefore, this study focuses on damage behaviour under high-energy impact loads, which needs further insight. Some work is also presented on fibre metal laminates yet effect of placing a ceramic sandwich core in between laminates is a new aspect to this research. The effect of increasing the cohesive interface area on energy absorption of structure when subject to high rate of loading is also investigated as part of this study [18].

Chapter 3

3. Mathematical Modelling

3.1 Empirical Model

Based on the experimental data available in literature, empirical relations are developed to exhibit the effect of strain rate on dynamic parameters under dynamic compression loading which is also the case in impact loading.

Dependency of dynamic parameters during in plane compression loading on impact pressure and strain rate is described with the help of present empirical equations. First, impact pressure will be used to define strain rate in terms of it and then the remaining parameters will be described in terms of strain rate. In-plane compression tests in SPHB (split pressure Hopkinson bar) showed that load vs time and velocity vs time graphs show two peaks after reaching a certain value of strain rate. And it is noted that first peak corresponds to matrix cracking (damage initiation) and second peak is related to delamination. [19]Onward linear curve shows the fast damage propagation and strain accumulation. As we know that, delamination is critical in fibre reinforced composite materials. Hence, it is very critical to investigate the dynamic parameters such as young's modulus E, peak pressure P and maximum stress σ. Based on the trends observed from experimental data, non-linear strain rate dependent evaluative constitutive relations developed using linear regression technique for these dynamic parameters are as follows:

$$\dot{\epsilon} = \{502.7 \times \ln(\dot{\epsilon})\} - 4.813$$

$$E = 6427.9\, e^{0.0026\dot{\epsilon}}$$

$$\sigma_{max} = 38.495\ \dot{\epsilon}^{0.26}$$

$$P_1 = 0.0013 \times \dot{\epsilon}^{0.27}$$

$$P_2 = 0.0025 \times \dot{\epsilon}^{1.31}$$

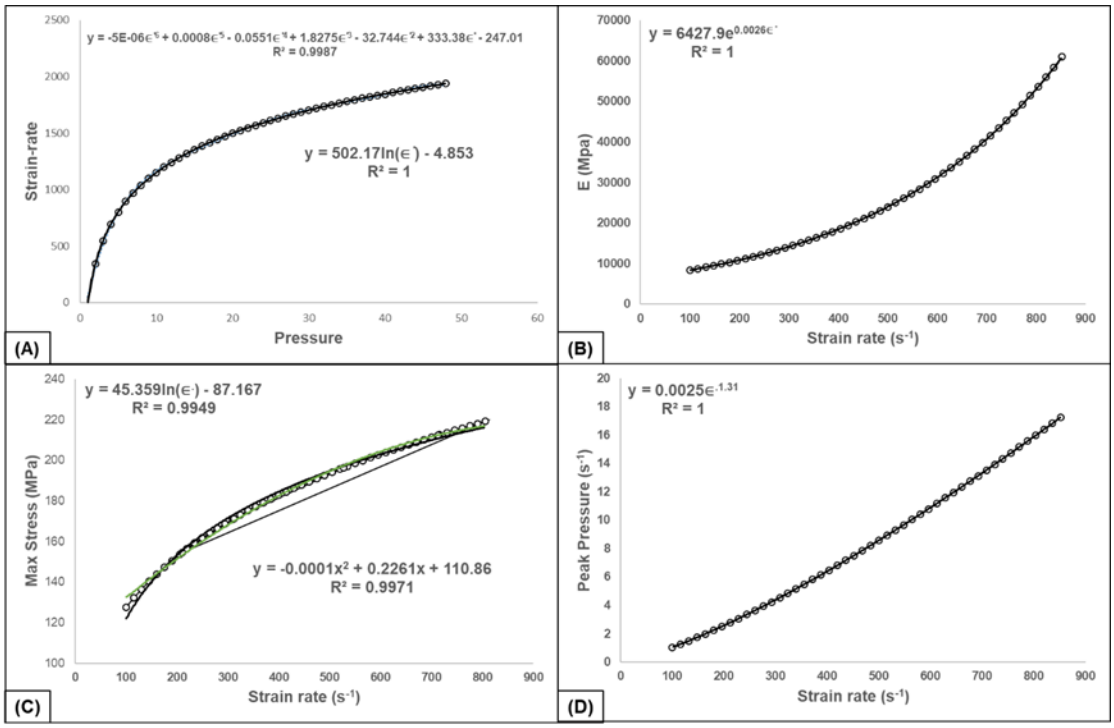

Fig. 3-1 Pressure Vs. Strain Rate

The results obtained using these empirical relations are in well correlation with the experimental results in literature [, as indicated from the above trends. It is clearly indicated from the graphs that mechanical properties are greatly influenced with the rate of loading. Exponential relation between strain rate and stiffness of the bonded joints indicates that the high strain rate loading renders the material behaviour to be more brittle. Therefore, a significant increase in strength and stiffness of the material is observed due to brittle nature of materials under high strain loading and the same is observed in literature.

3.2 Analytical Model

3.2.1 Damage Initiation

Failure in composite material is a complicated phenomenon and is dependent on many different parameters such as constitute properties, loading conditions, manufacturing processes, fibre fraction etc. all these factors influence the behaviour of laminated structure under load. Usually there are to analyse the failure of composite material: strength-based analysis and energy-based analysis.

Strength based analysis involves the determination of stresses and strain using some mathematical manipulations based on laminate theory, for a UD laminate, as follows:

$$\begin{Bmatrix}\sigma_l\\ \sigma_t\\ \tau_{lt}\end{Bmatrix}=\begin{bmatrix}\frac{E_l}{(1-\nu_{lt}\nu_{tl})} & \frac{\nu_{tl}E_l}{(1-\nu_{lt}\nu_{tl})} & 0\\ \frac{\nu_{lt}E_l}{(1-\nu_{lt}\nu_{tl})} & \frac{E_t}{(1-\nu_{lt}\nu_{tl})} & 0\\ 0 & 0 & G_{lt}\end{bmatrix}\begin{Bmatrix}\varepsilon_l\\ \varepsilon_t\\ \gamma_{lt}\end{Bmatrix}$$

This can be formulated as below in terms of elastic coefficients:

$$\begin{Bmatrix}\sigma_l\\ \sigma_t\\ \tau_{lt}\end{Bmatrix}=\begin{bmatrix}\bar{E}_l & \nu_{tl}\bar{E}_l & 0\\ \nu_{lt}\bar{E}_t & \bar{E}_t & 0\\ 0 & 0 & G_{lt}\end{bmatrix}\begin{Bmatrix}\varepsilon_l\\ \varepsilon_t\\ \gamma_{lt}\end{Bmatrix}$$

$$[\sigma]_{lt}=C[\varepsilon]_{lt}$$

Stiffness matrix is used to link local stress with local strains and using the above relationship local stresses can be obtained from local strains which are obtained experimentally using strain gauges.

Local stresses obtained from equation (3.6) & (3.7) are the stress along longitudinal and transverse fibre direction in the plane of laminate. Whereas, to apply strength-based criteria we need to calculate the global stresses with reference to global coordinate system of the complete structure.

Global stresses can be obtained from local stresses using a simple transformation matrix.

$$\begin{Bmatrix}\sigma_x\\ \sigma_y\\ \tau_{xy}\end{Bmatrix}=\begin{bmatrix}c^2 & s^2 & 2cs\\ s^2 & c^2 & -2cs\\ -cs & cs & (c^2-s^2)\end{bmatrix}\begin{Bmatrix}\sigma_l\\ \sigma_t\\ \tau_{lt}\end{Bmatrix}$$

$$[\sigma]_{xy}=[T_1][\sigma]_{lt}$$

Where $[T_1]$ is the transformation matrix.

$$\begin{Bmatrix}\varepsilon_l\\ \varepsilon_t\\ \gamma_{lt}\end{Bmatrix}=\begin{bmatrix}c^2 & s^2 & -cs\\ s^2 & c^2 & cs\\ 2cs & -2cs & (c^2-s^2)\end{bmatrix}\begin{Bmatrix}\varepsilon_x\\ \varepsilon_y\\ \gamma_{xy}\end{Bmatrix}$$

$$[\varepsilon]_{lt} = [\dot{T_1}][\varepsilon]_{xy}$$

As we know that,

$$[\dot{T_1}] = [T_1]^{-1} = [T_1]^t$$

Where t is transpose of matrix.

Therefore,

$$\begin{Bmatrix} \sigma_x \\ \sigma_y \\ \tau_{xy} \end{Bmatrix} = [T_1] \begin{bmatrix} \bar{E}_l & \nu_{tl}\bar{E}_l & 0 \\ \nu_{lt}\bar{E}_t & \bar{E}_t & 0 \\ 0 & 0 & G_{lt} \end{bmatrix} [\dot{T_1}] \begin{Bmatrix} \varepsilon_x \\ \varepsilon_y \\ \gamma_{xy} \end{Bmatrix}$$

$$[\sigma]_{xy} = [T_1][C][\dot{T_1}][\varepsilon]_{xy}$$

Using the above set of equations, we can calculate the global stresses which can now be used in strength-based criteria to predict the failure of composite laminate.

There are various failure criteria available in literature and most common of them are:

- Hashin Damage Criteria
- Tsi-Wu Criteria
- Puck Criteria
- Hill Criteria

Most widely used of these is Hashin damage criteria.

Fibre Tension Failure ($\sigma_{11} \geq 0$):

$$\left(\frac{\sigma_{11}}{X^T}\right)^2 + \frac{\sigma_{12}^2 + \sigma_{13}^2}{S_{12}^2} = \begin{cases} \geq 1 \,; Fail \\ < 1 \,; Safe \end{cases}$$

Fibre Compression Failure ($\sigma_{11} < 0$):

$$\left(\frac{\sigma_{11}}{X_C}\right)^2 = \begin{cases} \geq 1 \,; Fail \\ < 1 \,; Safe \end{cases}$$

Matrix Tension Failure ($\sigma_{22} + \sigma_{33} \geq 0$):

$$\left(\frac{\sigma_{22} + \sigma_{33}}{Y^T}\right)^2 + \frac{\sigma_{23}^2 + \sigma_{22}\sigma_{33}}{S_{23}^2} + \frac{\sigma_{12}^2 + \sigma_{13}^2}{S_{12}^2} = \begin{cases} \geq 1 \,; Fail \\ < 1 \,; Safe \end{cases}$$

Matrix Compression Failure ($\sigma_{22} < 0$):

$$\left[\left(\frac{Y_C}{2S_{23}}\right)^2 - 1\right]\left(\frac{\sigma_{22}+\sigma_{33}}{Y_C}\right) + \frac{(\sigma_{22}+\sigma_{33})^2}{4S_{23}^2} + \frac{\sigma_{23}^2 - \sigma_{22}\sigma_{33}}{S_{23}^2} + \frac{\sigma_{12}^2 + \sigma_{13}^2}{S_{12}^2} = \begin{cases} \geq 1\,; Fail \\ < 1\,; Safe \end{cases}$$

Considering the above-mentioned relations, it is depicted that the strength-based failure criteria are only suitable to show damage onset for different failure mechanism. They are not able to track the growth or propagation of damage modes which is very critical in case of composite materials due to their unpredicted nature of failure. Therefore, to observe damage propagation it is important to perform experiments which give us an insight to material failure behaviour especially in case of fibre fracture. However, it is very difficult to analyse matrix failure or interface failure and only way possible to do this is finite element analysis. It is cost efficient tool to trace damage evolution on which this study mainly aims to focus on.

3.3 Energy Absorption

Energy absorbed by Alumina Layer:

As the impact event progresses, the ceramic layer is subjected to compressive as well as tensile loading. If the allowable limit is breached by compressive stresses, the ceramic will fail in compression.

The energy density absorbed due to compression of sandwich core is:

$$E_c^c = \int_0^{\epsilon} \sigma_c^c . \epsilon_c^c . d\epsilon$$

As the impactor strikes the ceramic, friction would be generated between the impactor and ceramic, as well as the ceramic would be broken into tiny pieces. Gailly et al. explained the process of formation of tiny pieces from the ceramic plate as pulverization.

Energy absorbed by Kevlar:

During the impact event, Kevlar fibre layer would fail due to elastic deformation, fibre tensile failure and delamination.

Primarily, the Kevlar layer will experience elastic deformation due to bending. When the strain in the impact zone crosses failure strain, the fibres will fail due to tension.

Energy density absorbed by Kevlar layer due to elastic deformation (bending) is given as:

$$E_{def}^{kev} = \int_0^{\epsilon} \sigma_s^{kev} . \epsilon_s^{kev} . d\epsilon^{kev}$$

Energy density absorbed by Kevlar layer due to tensile failure of fibre is given as:

$$E_{tf}^{kev} = \int_0^{\epsilon_o^{kev}} \sigma^{kev} . \epsilon^{kev} . d\epsilon^{kev}$$

Energy absorbed in Delamination.

Delamination energy can be determined by damage area analysis. When a composite laminate is subjected to impact load, delamination will start below the impact region and with increased impact energy delamination area also broadens [20]. Matrix cracking also happens at this point and many studies concluded that matrix cracking is the reason for delamination and only delamination energy needs to be calculated. It needs to be pointed out that matrix cracking does involve energy dissipation, but it is negligible as compared to delamination energy. Delamination area can be estimated using deeply technique or digimat and energy absorbed in delamination can be determined as follows:

$$E_{del} = K . \sum_{i=1}^{n-1} A_i$$

Where,

E_{del}: delamination energy

K: fracture toughness under impact

A_i: delaminated area in i^{th} layer

n: number of plies

Generally, the matrix cracking area is same is delamination.

$$E_{mc} = \sum_{i=1}^{n-1} A_i e_m V_m$$

Where,

e: matrix cracking energy per unit volume

V_m: Volume fraction of matrix

Finally, the total energy absorbed in impact is the sum of elastic deformation energy, fibre failure energy and delamination energy.

$$E_{Total} = E_{reb} + E_{def} + E_{tff} + E_{del}$$

Energy absorbed in fibre failure.

Total energy of the impactor is sum of kinetic and potential energy.

$$E_T = K.E + P.E$$

As we know that,

$$K.E = \frac{1}{2}mv^2$$

$$P.E = mgh$$

Where,

m: mass of impactor

v: velocity of impactor

h: height of impact

Starting with velocity of 2 ms^{-1}

$$K.E = \frac{1}{c}(1.2)(2)^2 = 2.4\,J$$

$$P.E = (1.2)(9.81)(0.005) = 0.058J$$

As height of impact is very small, hence potential energy is very small as compared to kinetic energy and can be neglected.

Finally,

Energy before impact = 2.4 J

Fibre fracture energy can be calculated simply using fracture toughness under impact and fracture area.

$$E_{ff} = K.\sum_{i=1}^{n-1} A_f^i$$

Assuming that fibre failure occur along transverse direction at 90o, we can calculate an estimated fracture area using simple mathematical formulation. Then, using the above equation, we can calculate energy absorbed in fibre failure.

$$Fracture\ Area\ for\ kevlar\ Layer\ 1 = F.A_{layer\ 1} = 1.1752 \times 10^{-4}\ m^2$$

$$F.A_{layer\ 1} = F.A_{layer\ 2} = F.A_{layer\ 3} = F.A_{layer\ 4}$$

$$Fracture\ Area\ for\ Core = F.A_{core} = 1.4691 \times 10^{-4}\ m^2$$

Using this area with fracture energy per unit area, we get energy absorption for fibre failure. However, it is important to note that this energy dissipation as indicated by graph below is very

small as compared to delamination damage energy. To calculate delamination damage energy, we need to calculate damage area as in the case of fibre failure. But there is no such way to calculate damage area analytically and it is dependent on experimentation or simulations. Therefore, numerical simulation are performed to determine the total damage dissipation energy, which is the sum of matrix cracking (very small), fibre failure and delamination damage energy (highest of all) dissipation.

Table 3-1. Energy Dissipation in fibre failure determined at 3 points for each layer along thickness direction

	Measurement Point	**Remaining Kinetic Energy**
Kevlar Layer 1	1	2.4
	2	2.25
	3	2.1
Kevlar Layer 2	4	2.1
	5	1.95
	6	1.8
Core	7	1.8
	8	1.72654
	9	1.653
Kevlar Layer 3	10	1.653
	11	1.50309
	12	1.35309
Kevlar Layer 4	13	1.35309
	14	1.20309
	15	1.05309

The data shown in the above table has been graphically represented on the next page.

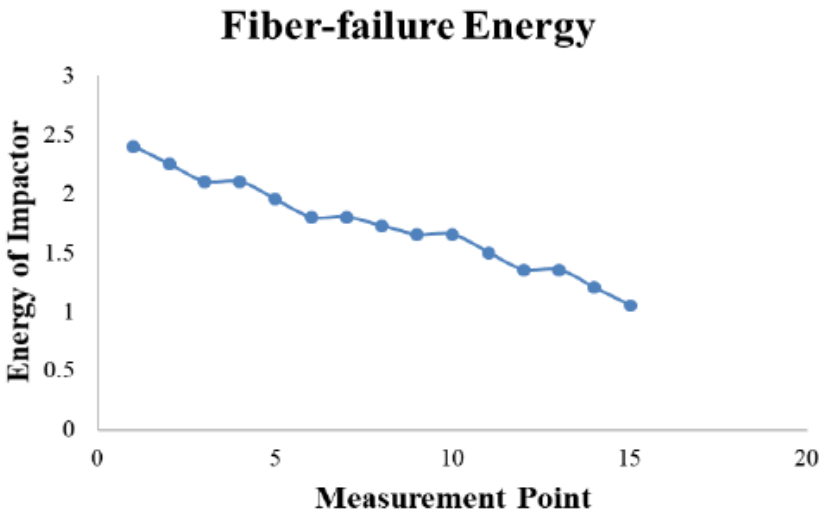

Fig. 3-2 Energy Dissipation in fibre failure determined at 3 points for each layer along thickness direction

Chapter 4

4. Model Design & Numerical Modelling

4.1 Core Thickness

First of all, we need to calculate the core thickness for the development of numerical model. For this purpose, we have used some commercially available helmet as reference for values of dimension and mass keeping in view the practicable application of this study. Parameters of available helmet are as follows:

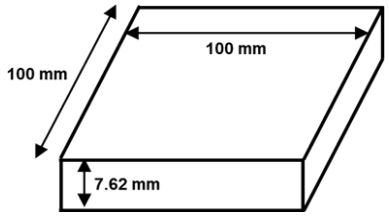

$$Length = Width = 100\ mm$$

$$Thickness = 7.62\ mm$$

$$Material = Kevlar - 49$$

$$Density\ of\ Kevlar = \rho = 1440\ kgm^{-3}$$

$$Volume = V = 100 \times 100 \times 7.62 = 7.62 \times 10^{-5}\ m^3$$

As we know that,

$$Mass = Density \times Volume$$

$$\boldsymbol{Mass\ of\ Kevlar\ Sheet = 0.109728\ kg}$$

The value of mass for Kevlar sheet of thickness 7.62 mm (thickness of commercially available helmet) works as reference for us to calculate the thickness of sandwich ceramic core. As we are using four layers of Kevlar, 2 on each side of core, of thickness 1mm. Hence,

$$Mass\ of\ one\ layer\ of\ kevlar = m = 0.0144\ kg$$

$$Mass\ of\ Kevlar\ layers = 4 \times 0.0144 = 0.0576\ kg$$

$$Mass\ of\ Core = 0.109728 - 0.0576$$

$$m_{Al} = 0.05212$$

$$Density\ of\ Alumina = \rho = 3900\ kgm^{-3}$$

As we know that,

$$\boldsymbol{Volume = \frac{Mass}{Density} = \frac{0.05212}{3900} = 1.3366 \times 10^{-5} m^3}$$

Using the relation between volume, area and thickness, we have

$$Volume = Area \times Thickness$$

$$Area = 0.1 \times 0.1 = 0.01\ m^2$$

$$\boldsymbol{Thickness = \frac{Volume}{Area} = \frac{1.3366 \times 10^{-5}}{0.01} = 1.3366 \times 10^{-3}\ m}$$

$$\boldsymbol{Thickness\ of\ Alumina\ Sheet = t = 1.33\ mm}$$

The thickness of the ceramic core comes out to be 1.33mm. It is decided to use a thickness little less than this value as we want the weight of this developed sheet (comprised of Kevlar layers and sandwich core) not to exceed the weight of corresponding sheet of commercially available helmet. Therefore, we have used a 1.25 mm thickness for Alumina core sandwiched between composite layers.

4.2 Modelling of Alumina Core

It is desired to increase the interface area of core. The interface area in contact with composite layers cannot be increased without except that the overall dimension of the sandwich core is

altered. Hence, it is decided to model the same rectangular core using the smaller tiles of different shapes and as a result we can increase the interface area without increasing the overall dimensions of core. Calculations of area and other dimensions of different tile shapes are as follows:

4.2.1 Square Tile

To start off, we have assumed a cell size of 13x13 mm^2 for square cell.

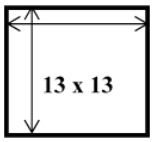

$$Length = L = 13\ mm$$

$$Width = W = 13\ mm$$

$$\boldsymbol{Area = A = 13 \times 13 = 169\ mm^2}$$

The surface area for square tile comes out to be 169 mm^2. Now all the other tiles must have an equivalent surface area to this.

Table 4-1. Dimensional parameters for different tiles shapes of sandwich core

	Square Tiles
Dimension of Sides (mm)	13
Surface Area (mm^2)	169
Interface Area (mm^2)	1820

4.3 Modelling Methodology

The finite element model for the simulation of impact analysis of Kevlar-Alumina-Kevlar sandwich structure for different impact velocities is created using a commercial FE modelling software ABAQUS/Explicit. Composite laminates are modelled using in-plane continuum shell elements, core is analysed using 3D stress elements and the indenter is considered as rigid body

with infinite rigidity and modelled as such, with the assumption that there is little or no deformation during the impact. Hashin failure criteria is used to predict different intra-laminar failures of composite plies; whereas to characterize the delamination and inter-laminar damage behaviour, cohesive zone modelling with the implication of traction-separation law is characterize the delamination and inter-layer damage behaviour. Cohesive surface is used to represent the interface between the layers.

4.4 Modelling

Model consists of an Alumina core (Thickness= 1.25mm; Area= 100x100 mm^2) sandwiched between two layers of Kevlar (Thickness= 1mm; Area= 100x100 mm^2) on both sides of sandwich core arranged as:

[Kev-(-45^o) / Kev-(+45^o) / Alumina Core / Kev-(+45^o) / Kev-(-45^o)]

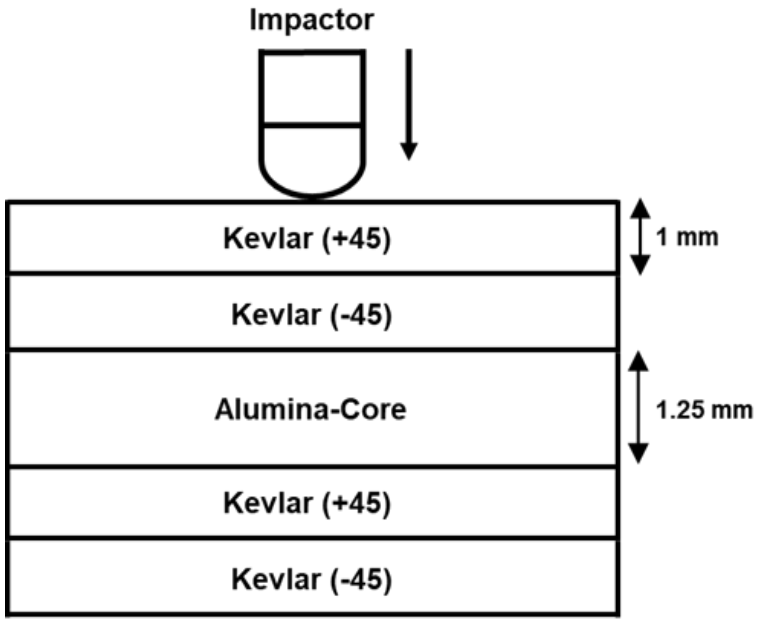

Figure 4-1. Schematic Diagram of model

All the components are modelled and assembled using ABAQUS 6.13 according to dimensions.

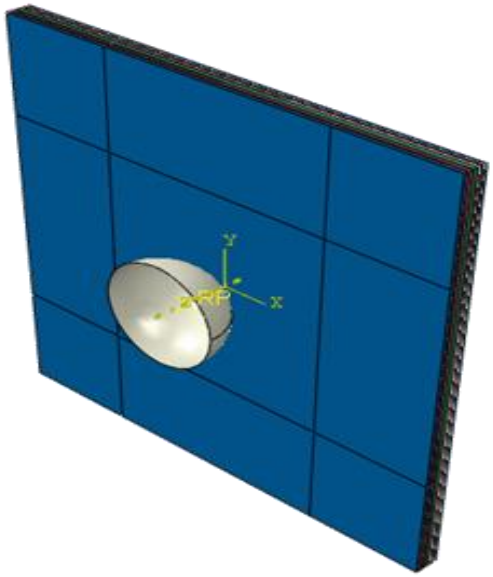

Figure 4-2. ABAQUS Assembly Model

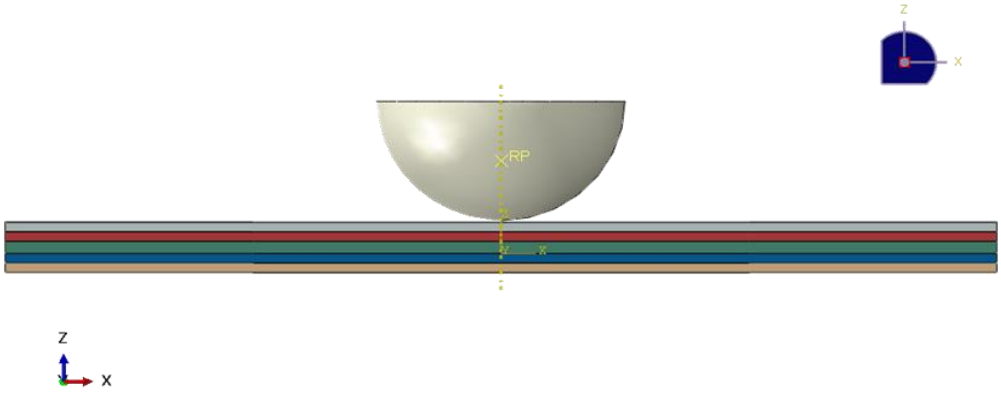

Figure 4-3. ABAQUS part instance model

4.5 Modelling of Alumina Core

It is desired to increase the interface area of core. The interface area in contact with composite layers cannot be increased without except that the overall dimension of the sandwich core is altered. Hence, it is decided to model the same rectangular core using the smaller tiles of different shapes and as a result we can increase the interface area without increasing the overall dimensions of core. Four scenarios sandwich core have been modelled using equivalent area concept. These are named as.

- Solid Core (S-Core)
- Square Tiles Core (ST-Core)

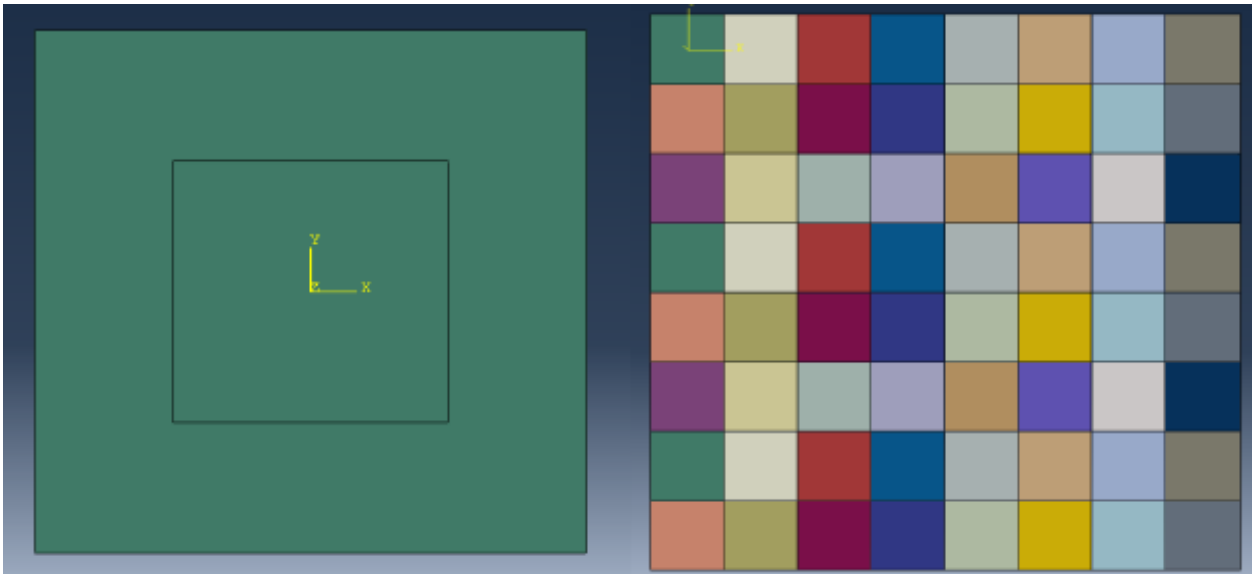

Figure 4-4. Part instance models of the two cases. Solid core (left). ST core (Right)

4.6 Damage Modelling

4.6.1 Delamination Damage Behaviour (Traction-Separation Law)

There are different methods for delamination modelling mainly based on two approaches:

Fracture Mechanics Approach

Virtual crack closure technique (VCCT)

- J-Integral methods
- Virtual crack extension method
- Stiffness derivative

Damage Mechanics Approach

- Cohesive element modelling
- Cohesive zone modelling (CZM)

Inter-laminar failure (Delamination) is modelled using cohesive zone damage formulation. In this approach, damage onset is determined using stress based analysis method whereas damage mechanics is employed for predicting damage propagation. There are two different ways to model the cohesive zone at the interface of two layers in ABAQUS solver. First, continuum cohesive element is setup at the interface of different layers. It is necessary to define the interaction properties between adjacent layers and cohesive element. Due to this reason, some finite thickness be defined for these cohesive elements along with two distinct faces.

Second, cohesive zone can be modelled by defining a surface based cohesive interaction between adjacent layers. Later allows the specification of traction-separation behaviour for surfaces. The second method is mostly used for interfaces with very small dimension in thickness direction. Computational time increases significantly due to determination of stable time increment of the complete model due to very small thickness of cohesive elements (usually in microns). Secondly, the progressive damage modelling is used to simulate cohesive element failure behaviour, which leads to convergence difficulties due to softening in the material response. Considering the advantages of surface type cohesive behaviour approach in modelling the delamination damage in comparison with cohesive elements, surface based cohesive interaction behaviour is utilized to model the delamination damage behaviour at the interface of different layers in this study. Cohesive surface behaviour requires traction-separation law to incorporate linear elastic behaviour at the initial stage to be followed by a damage onset and propagation. The elastic constitutive matrix can be used to explain the elastic regime. The stress vector due to traction has three components.

- t_n, t_s (for 2D problems represent shear tractions)
- t_t (in 3D problems along with other two represent normal traction along 3-direction)

The deflections are represented as: δ_n, δ_s, and δ_t. The uncoupled elastic behaviour is expressed as following:

$$t = \begin{Bmatrix} t_n \\ t_s \\ t_t \end{Bmatrix} = \begin{bmatrix} K_n & 0 & 0 \\ 0 & K_s & 0 \\ 0 & 0 & K_t \end{bmatrix} \begin{Bmatrix} \delta_n \\ \delta_s \\ \delta_t \end{Bmatrix} = K\delta$$

When the damage initiation criteria specified in material model is satisfied at some contact point, the degradation begins at that point. The quadratic stress failure criterion is employed, in this numerical study, to determine the damage onset of inter-laminar failure at the interface of different plies. Quadratic interaction function developed using contact stress ratios is used to interpret damage initiation. The damage begins to initiate as the value of the above-mentioned quadratic interaction function reaches to unity. Above mentioned criterion can be expressed as follows:

$$\left\{\frac{(t_n)^2}{t_n^o}\right\} + \left\{\frac{(t_s)^2}{t_s^o}\right\} + \left\{\frac{(t_t)^2}{t_t^o}\right\} = 1$$

Where t_i (i = n, s, t) is a stress vector due to traction at the interface. Value of 't' in the denominator represents the maximum value of traction stress. Also, n,s and t, subscripts in the numerator terms represent normal traction stress vector, shear stress traction in both the directions respectively.Once the damage initiation criterion is reached, cohesive stiffness starts to degrade at a certain rate. the damage evolution law defined in the material model determines the rate of degradation of cohesive zone stiffness. The overall damage at some contact point is represented by a scalar damage variable denoted as 'd'. Value of 'd' is zero till the damage initiation. In the damage progression phase, d progresses monotonically frim 0 to1. Traction stresses in both normal and shear direction are greatly affected as a result damage progression in the following manner:

$$\{t_n\} = (1-d)\bar{t_n}$$

$$\{t_s\} = (1-d)\bar{t_s}$$

$$\{t_t\} = (1-d)\bar{t_t}$$

Traction stresses on the right of the above equations are stresses calculated for undamaged specimen by the implication of elastic traction-separation behaviour.

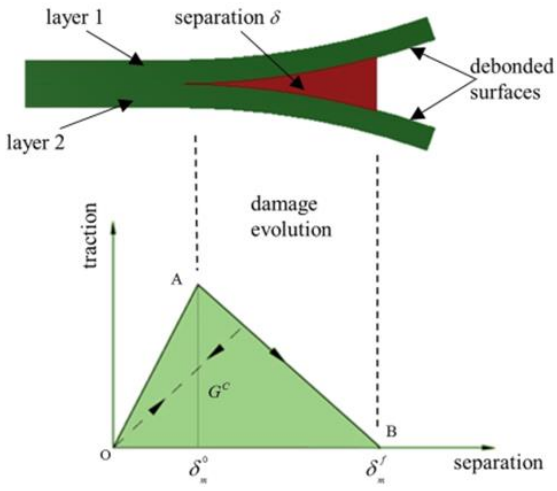

Figure 4-5. Cohesive Interface damage process with bi-linear traction

Linear loading-unloading behaviour is assumed always after the initiation of damage as show in fig. once the damage onset is reached, further loading leads to softening of materials as represented by line AB in figure.

Benzeggagh–Kenane proposed an energy based fracture criterion commonly known as 'B-K power law' and is used as damage evolution law in here can be expressed as follows[3]:

$$G_n^C + (G_s^C - G_n^C) + \left(\frac{G_s + G_t}{G_n + G_s + G_t}\right)^{\eta} = G^C$$

Where,

G = Fracture energy per unit area

η = Cohesive property parameter

'G^C' = Critical fracture energy.

4.7 Progressive Damage Model for Intralaminar Failure Mechanism

Failure analysis of fibre-based (FRP) composites requires damage characterization be performed before the process. Failure of FRP composites is considered as elastic-brittle type failure as there

is no significant plastic deformation can be observed during damage initiation phase. Hence, plasticity is totally neglected in the modelling of fibre-based composites allowing us to use inbuilt damage model for anisotropic material. The present numerical study is based on the studies of Hashin, Hashin and Rotem, Matzenmiller et al. and Camanho and Davila.

On the basis of following failure modes damage is distinguished:

- Fibre failure in longitudinal tension,
- Fibre kinking and buckling during longitudinal compression.
- Matrix failure under transverse tension/shearing
- Transverse compression/shearing

These four damage modes can be expressed as follows: (Hashin Damage Equations)

Table 4-2. Hashin Damage Equations

Fibre Tension ($\boldsymbol{\sigma_{11} \geq 0}$)	$F_f^t = \left(\frac{\widehat{\sigma_{11}}}{X^T}\right)^2 + \alpha\left(\frac{\widehat{\tau_{12}}}{S^L}\right)^2$
Fibre Compression ($\boldsymbol{\sigma_{11} < 0}$)	$F_f^c = \left(\frac{\widehat{\sigma_{11}}}{X^C}\right)^2$
Matrix Tension ($\boldsymbol{\sigma_{22} \geq 0}$)	$F_m^t = \left(\frac{\widehat{\sigma_{22}}}{Y^T}\right)^2 + \left(\frac{\widehat{\tau_{12}}}{S^L}\right)^2$
Matrix Compression ($\boldsymbol{\sigma_{22} < 0}$)	$F_m^c = \left(\frac{\widehat{\sigma_{22}}}{2S^T}\right)^2 + \left[\left(\frac{Y^C}{2S^T}\right)^2 - 1\right]\left(\frac{\widehat{\sigma_{22}}}{Y^C}\right) + \left(\frac{\widehat{\tau_{12}}}{S^L}\right)^2$

Where,

X^T: longitudinal tensile strength

X^C: the longitudinal compressive strength

Y^T: the transverse tensile strength

Y^C: the transverse compressive strength

S^L: longitudinal shear strength

S^C: compressive shear strength

α: contribution of shear stress in fibre tensile direction failure

$\widehat{\sigma_{11}}, \widehat{\sigma_{22}}, \widehat{\tau_{12}}$: components of stress tensor

Prior to the start of damage, plane stress stiffness matrix of orthotropic material determines the linear elastic behaviour of material represented as following:

$$\sigma = C_d \varepsilon$$

Where:

σ = True stress

ε True strain

C_d = Damaged elasticity matrix

Once the damage initiation criteria mentioned in equation is reached, as a result of damage propagation, material stiffness gradually decreases will the final fracture happens. Energy released during the damage process controls the damage propagation of the deteriorating material.

More detail about the damage initiation and evolution of the material can be found in Abaqus analysis user's guide[1], [4], [7]. Following the establishment of different relationships related to linear elastic material behaviour, damage onset and damage propagation of material, now is the time to define material removal. This is a significantly important step show perforation effect especially in impact related simulations. Element deletion from the mesh happens once either of damage variable reaches its peak value during an explicit dynamic analysis. Afterwards, the deleted element shows no further resistance to deformation. The strength and damage properties of Kevlar and Alumina used in this numerical study are mentioned below in the table.

Table 4-3. Material properties of Kevlar-49/Phenolic composite [8]

ρ	E_{11}	E_{22}	ν_{12}	G_{12}	G_{23}	G_{13}
Kgm^{-3}	**GPa**	**GPa**		**GPa**	**GPa**	**GPa**
1467	151.7	4.14	0.35	2.90	1.5168	1.5168

Table 4-4. Material properties of Kevlar-49/Phenolic composite [7]

X_t	X_c	Y_t	Y_c	S_{12}	S_{23}	$F.E_{(LT)}$	$F.E_{(LC)}$	$F.E_{(TT)}$	$F.E_{(TC)}$
MPa	**MPa**	**MPa**	**MPa**	**MPa**	**MPa**	**N/mm**	**N/mm**	**N/mm**	**N/mm**
2757.9	517.12	50.4	253	81	108	1.1	0.6	0.7	1.2

4.8 Discretization

4.8.1 Composite Laminates

A composite sandwich structure is modelled using Kevlar fibres and Alumina core. 2 layers of Kevlar (1 mm) are laid up at $+45^o$ and -45^o. Layup is symmetric in nature and Alumina core is placed in between the layers of Kevlar fibres at the center. Kevlar-49 phenolic is used in this case. Kevlar layers are modelled using 8-node brick (quadrilateral) continuum shell elements (SC38R), with reduced integration method being applied. Impact zone is meshed with an element size of $0.25\times0.25\times0.25$ mm^3 while mesh size of $0.5\times0.5\times0.5$ mm^3 is used for the remaining part of the ply. Stiffness relaxation is also applied to avoid hourglass of reduced integration elements having finite membrane strains. Each ply thickness is discretized using two elements. Friction Coefficient between two plies is set to 0.7 [2], [5]. Meshed model is shown below:

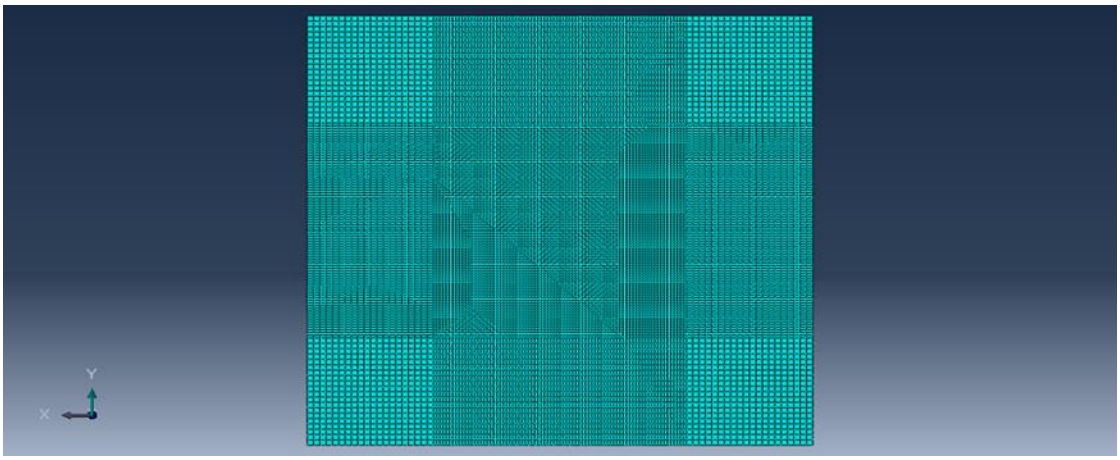

Figure 4-6. Kevlar layers are modelled using 8-node brick (quadrilateral) continuum shell elements (SC38R)

Lamina structures of small thicknesses can be very efficiently modelled using continuum shell elements instead of 3D solid elements with significantly low computational cost as compared to solid elements. Continuum shell elements do retain the predictive features required for 3D models of greater complexity. Therefore, continuum shell elements have been used in this study.

Moreover, solid elements do not behave well while undergoing effect as they experience shear locking and it is quite evident in our case that the composite structure is experiencing undergoing bending during the impact process. Also, more than one elements are required for the discretization of ply thickness in case of solid elements while only a single shell element is enough for thickness direction modelling[8]. Continuum shell elements can provide much improved through thickness response because of having a 3D geometric and stacking capability.

Continuum shell elements can cater for thickness changes in ply thickness direction because of having double sided contact as compared to conventional shell elements which are unable to do the above. Overall, continuum shell elements are much better for the modelling of thin laminated structures especially when dominated by bending behaviour as in the case of impact loading. Increase the impactor velocity will result in increased shear deformation. Hence, it is very important to select correct element type to avoid errors and to get accurate results [6], [9].

4.8.2 Discretization of Sandwich Core

Alumina core is discretized using 3D stress elements (3DS8R) with reduced integration and enhanced stiffness hourglass control being applied as well. 3D elements in this case are used to illustrate the damage progression in Alumina core as it will fail in brittle manner under impact. It is necessary for us to investigate the damage behaviour of Alumina core as it will play a crucial role in energy absorption.

The two scenarios for modelling of Alumina core have been mentioned as follows

- Solid Core
- Square Tiles Core

The complete meshed models of the square tile sandwich core models has been shown in figure below. In both of the cases the sandwich core is discretized using three elements in thickness direction to maintain aspect ratio close to 1 as required (discussed earlier) in case of impact related analysis. Moreover, cohesive zone modelling has been implied at the interface of different tiles to incorporate c.

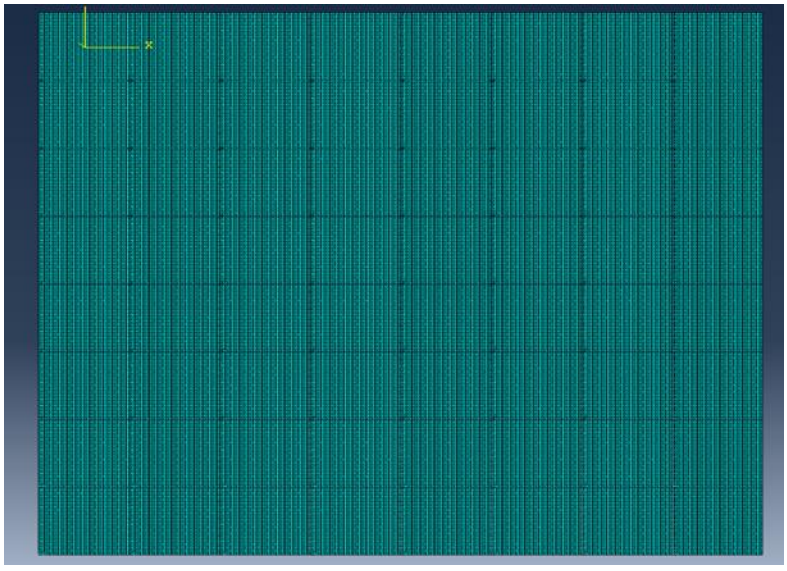

Figure 4-7. Square tile core meshed model

Meshing of second case i.e. solid core is same as that of composite laminate as shown in fig. Material properties of Alumina core are given in table.

Table 4-5. Material properties of Alumina

ρ	**E_{11}**	**E_{22}**	**ν_{12}**	**Fracture Strain**	**K_{IC}**	**G_{13}**
kgm^{-3}	**GPa**	**GPa**		**%**	**MPa/m^2**	**GPa**
3900	370	4.10	0.22	0.01	3.5	1.5168

4.9 Impactor

The impactor is considered to be as rigid body with infinite rigidity and modelled as such, with the assumption that there is little or no deformation during the impact. Hence, it is discretized using discrete rigid elements (4-node 3-D bi-linear rigid quadrilateral elements R3D4). Impactor is meshed with an element size of 0.25×0.25×0.25 mm^3 as the size of the impactor mesh elements needs to be compatible with the size of impact zone mesh elements to achieve smooth interaction between them. Moreover, the coefficient of friction between impactor and top ply is 0.3 [5].

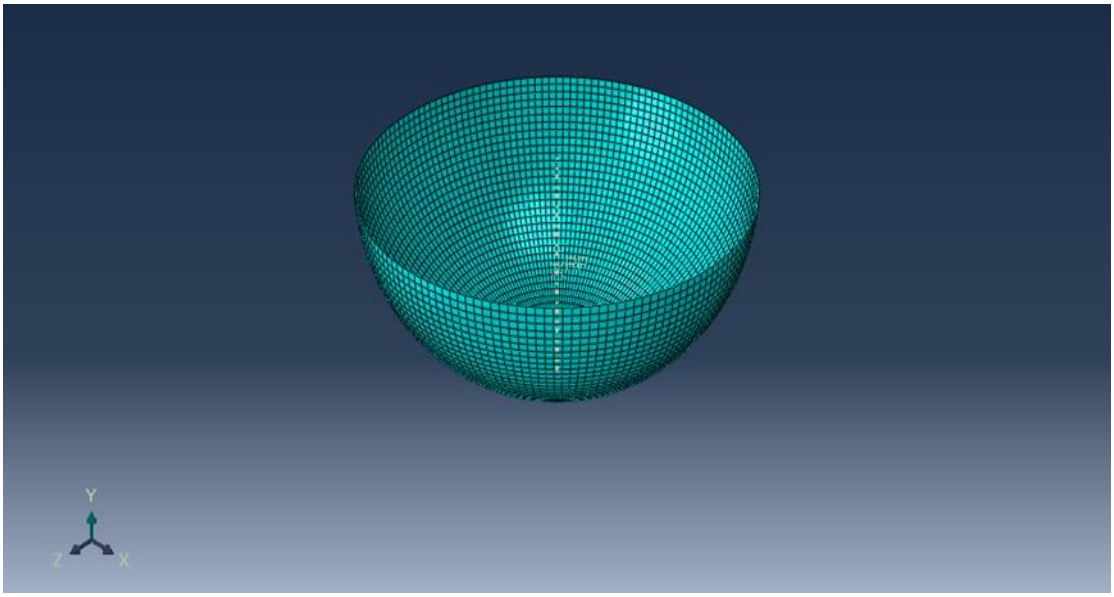

Figure 4-8. Impactor

4.10 Cohesive Zone Modelling

The adjacent plies are joined together using cohesive contact algorithm. Quadratic traction separation law is implied to predict delamination behaviour in between plies. The composite materials are modelled as orthotropic materials which indicates the linear elastic material behaviour before the damage onset.

Table 4-6. Material properties of Phenolic Resin (Properties of Cohesive Interface)

$K_n = K_n = K_n$	t_n^o	t_s^o	t_t^o	G_{IC}	G_{IIC}	G_{IIIC}	β
N/mm^3	MPa	MPa	MPa	N/mm	N/mm	N/mm	
10^6	230	115	115	0.7	1.1	1.15	1.45

4.10.1 Mesh Convergence

Mesh convergence study has been performed with different mesh size. A significant variation in the internal energy is observed for coarse mesh size as the big elements size contributes to the kinetic energy of the system. As mesh size is reduced energy absorption reduces and then stabilizes to certain value. Also, to ensure convergence stable time increment kept under above 1×10^{-8} sec. Mesh convergence plot between internal energy and no of elements is plotted as shown in figure. The model contains approximately around 400,000 elements and takes around 52 CPU hours to complete the task while running on Intel Xeon E5 2699 v3@2.30 GHz with 128 GB RAM.

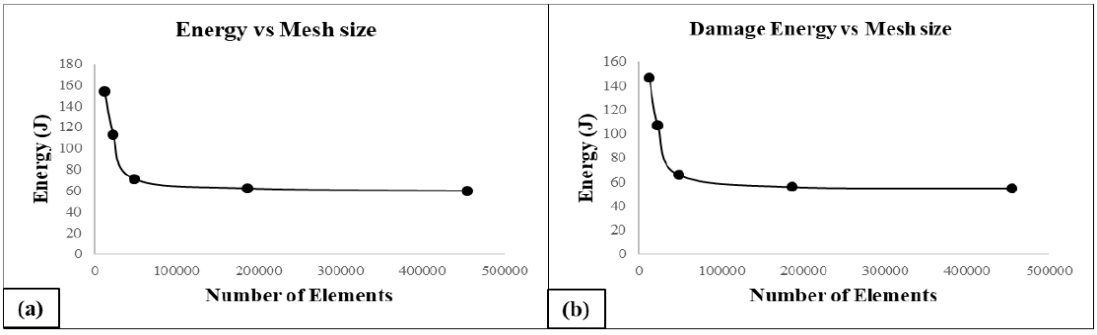

Figure 4-9. Convergence plots between energy and number of elements (a) Internal energy vs number of elements (b) Damage dissipation energy vs number of elements

Table 4-7. Complete meshing details

Part Name	Element Description	No. of Elements	A.R (Avg.)
Kevlar Lamina	Continuum Shell Elements: 8-node brick element (3DS8R)	85083	1.70
Impact Region	Continuum Shell Elements: 8-node brick element (3DS8R)	46875	1.20
Alumina Core	3D-Stress Solid Elements: 8-node brick element (3DS8R)	Alumina Core	
Impactor	Rigid Elements: 4-node quad element (R3D4)	6960	1.27
	Rigid Elements: 3-node tri elements	236	1.26
Square Tile	3D-Stress Solid Elements: 8-node brick element (3DS8R)	3072	1.03

4.11 Model Validation

It is necessary to compare the numerical solution with some experimental or analytical results for its validation. As this study consists of only mathematical model and numerical simulations and does not include experimentation. Also, it is not possible to calculate damage energy dissipation analytically because delamination damage area and matrix degradation pattern cannot be calculated analytically. Keeping in view the above stated problem, some evidence needs to be provided to prove the validation of our finite element model. Therefore, we used our model for simulation of results already published in literature for a similar type of dynamic analysis. Results of our model are in well correlation with the results of reference literature. Comparison of results are as follows:

Table 4-8. Comparison of absorbed energy of present model with reference model

Impact energy (J)	Absorbed energy (J)		Difference (%)
	Present Model	Reference Model	
5	2.664	3.43	22.4
10	5.328	6.34	15.9
15	10.313	11.43	9.77

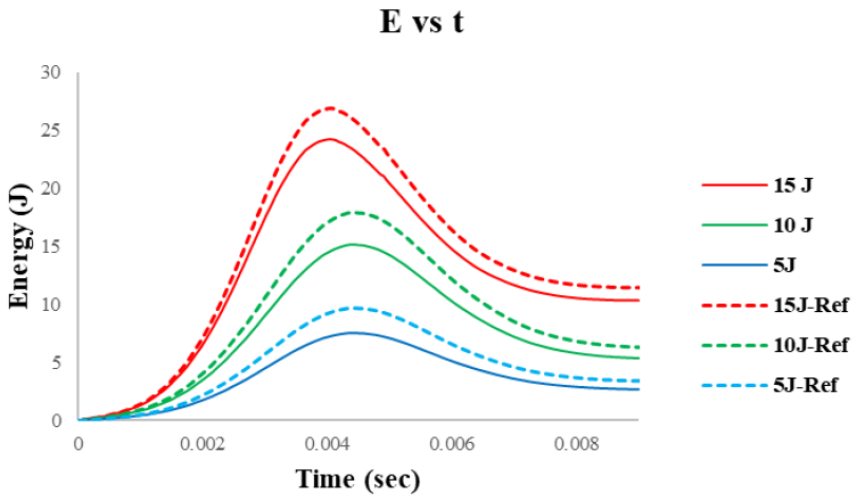

Figure 4-10. Internal energy vs time indicating absorbed energy for comparison with reference model

Chapter 5

5. Results and Discussion

5.1 Experimental Results

Experiments are performed to obtain the value of G_{IC} for ZTA and Kevlar. The tests were performed on the UTS machine and the plots for each of the tests have been shown in the figures below.

5.1.1 Tensile Testing

The Kevlar and phenolic based composite materials are subjected to tensile testing on the UTS machine. The Force displacement curves are plotted for each sample.

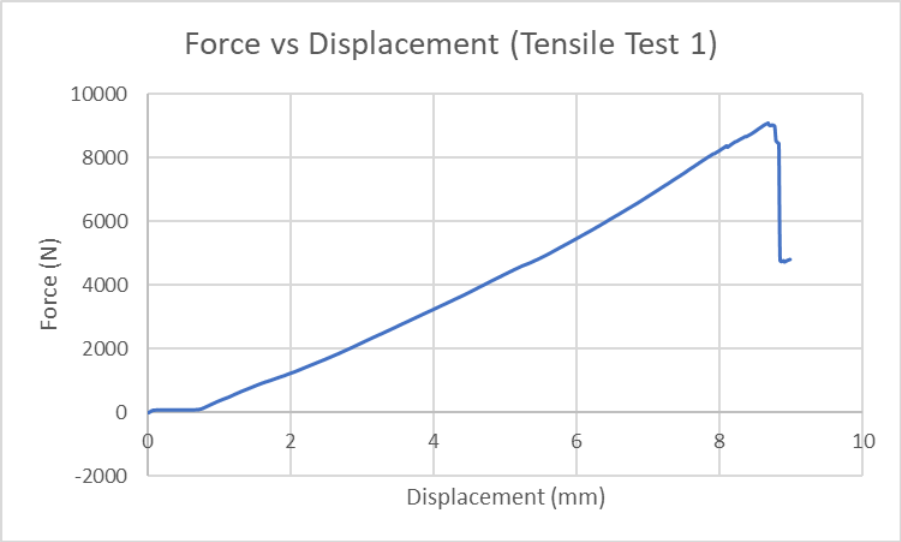

Fig. 5-1 Force displacement Curve for 1st Sample

Samples are fixed in the machine jaws and subjected to automatic loading; the peak force applied on the sample before failure is 9000 N.

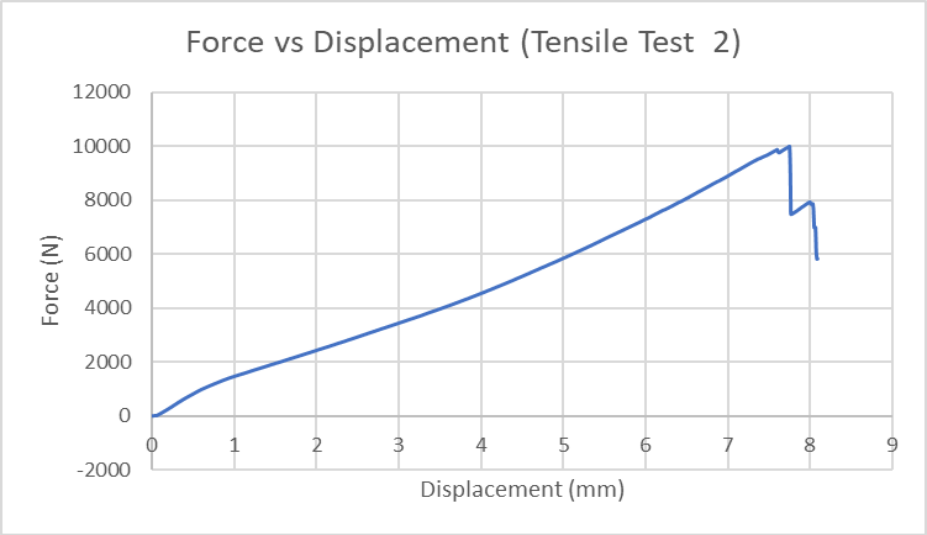

Fig. 5-2 Force displacement Curve for Sample 2

In the same way other samples are tested for their Ultimate tensile strength and Young's Modulus. The applied load and displacement data is further utilized in calculation of stress and strain for the specimen.

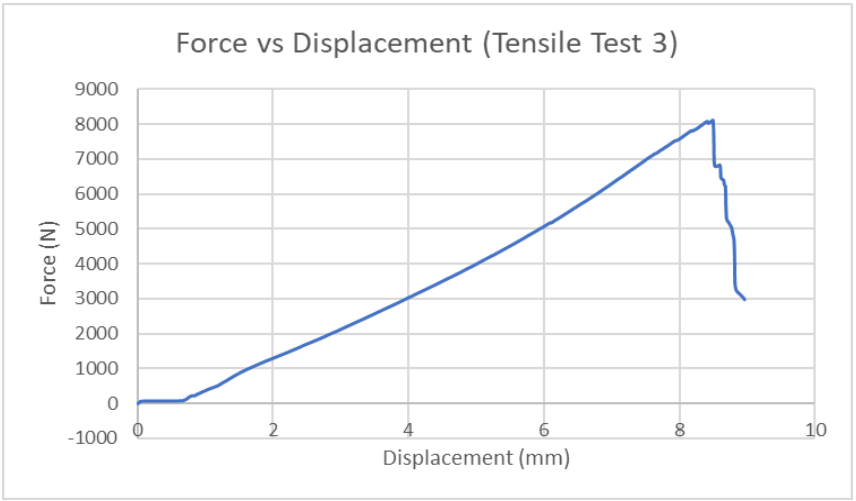

Fig. 5-3 Force displacement Curve for Sample 3

The comparison between the results of all three samples shows that the peak loading force is between 8000 N to 10000 N before failure which is very high. The displacement before the material failure is about 8 mm which could be due to material ductile nature or slippage of specimen in clippers of the Universal Tensile Testing Machine.

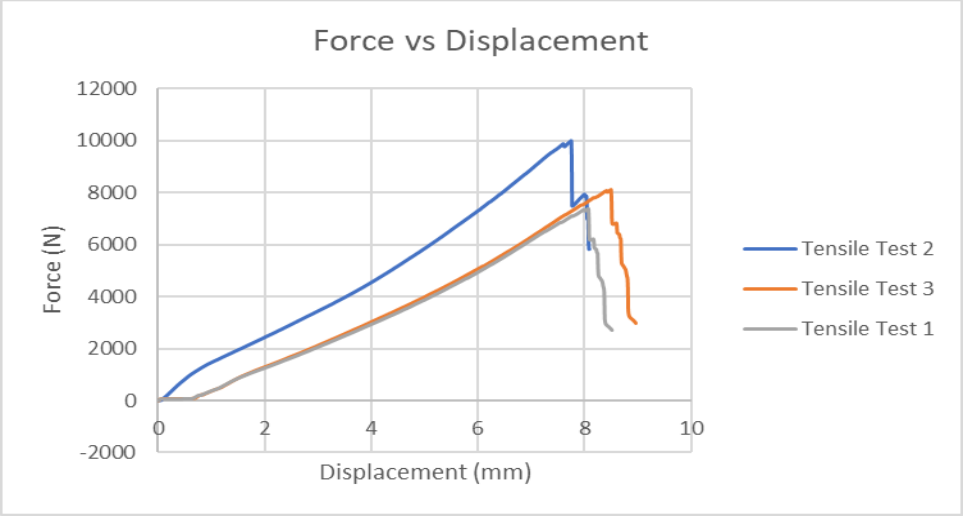

Fig. 5-4 Comparison of Tensile strength of samples

5.1.2 ZTA

Peel testing is performed with Kevlar and ZTA samples. The Results shows the force vs displacement curve for the test. The maximum force before the significant strain or delamination is about 60 N.

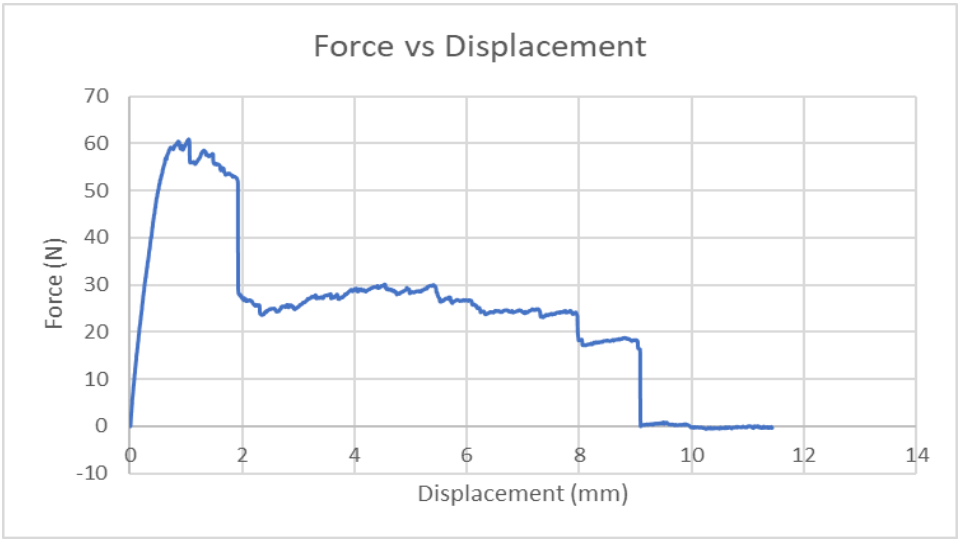

Fig. 5-5. Force Displacement Curve for ZTA-Kevlar Peel Test

5.1.3 Peel Testing

Peel testing enables precise assessment of sealing, painting, and adhesive efficiency and gives invaluable knowledge to overcome adhesive failure failure investigation and improve processing parameters.

Seals, laminates and adhesives for several purposes have been designed. In order to ensure that the product is safe to use and complies with anticipated requirements while maintaining the brand name, it is crucial to consider product performance and manufacturing parameters such as the adhesive application and curing.

Peel tests are performed on the samples made from Kevlar fibres and phenolic resin. The composite material is subjected to peel test to determine the strength of the material which is useful in low and high energy impact test modelling of the composite material.

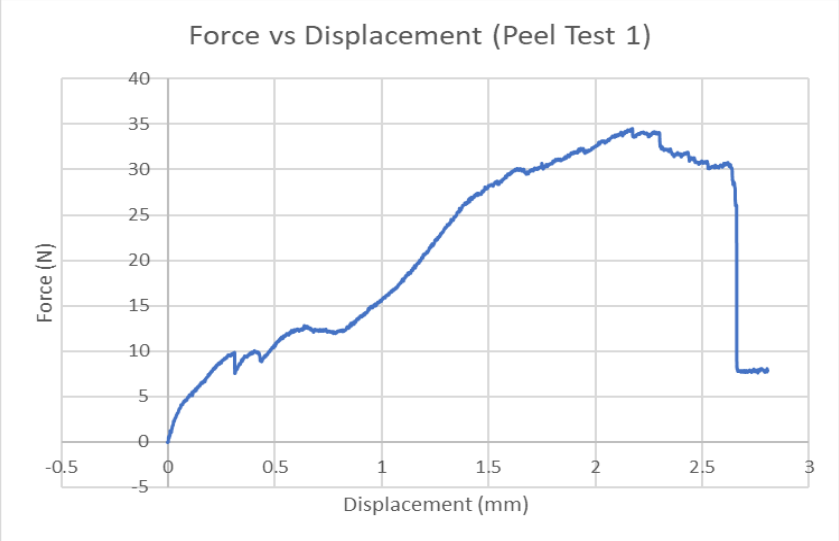

Fig. 5-6 Force displacement Curve for Sample 1

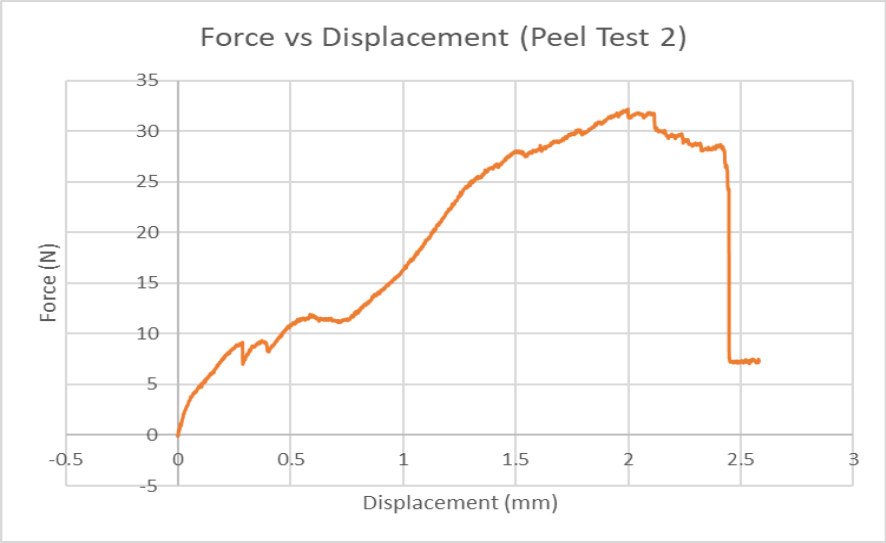

Fig. 5-7 Force displacement Curve for Sample 2

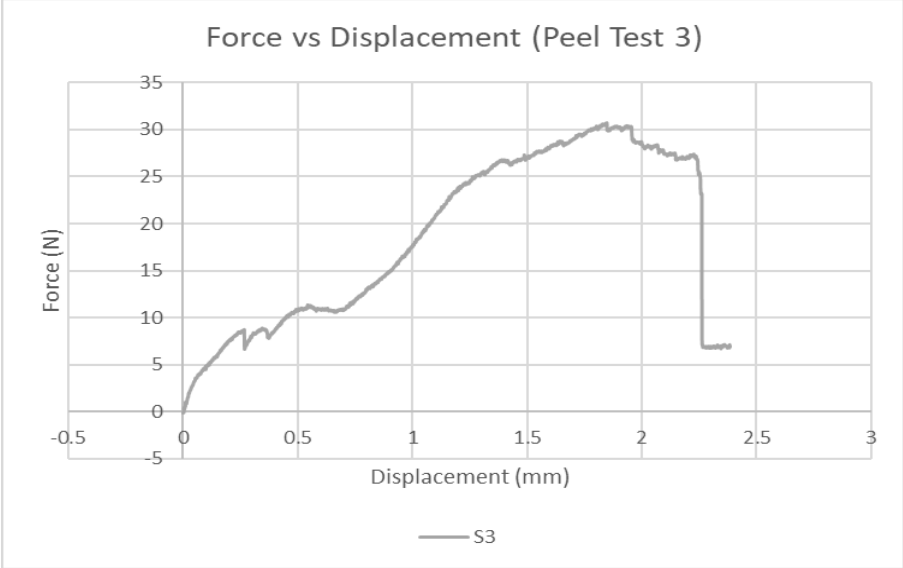

Fig. 5-8 Force displacement Curve for Sample 3

In the figure below, comparison of the peel tests for each sample is presented. The results show that the minimum load before the complete delamination of the composite layers is 30 whereas the maximum load is 34. In the same way the strain values are also close. The results lie in the short range which shows that the sample possess almost uniform mechanical properties. The average results are utilized in further research using the FEA model and low and high energy impact testing.

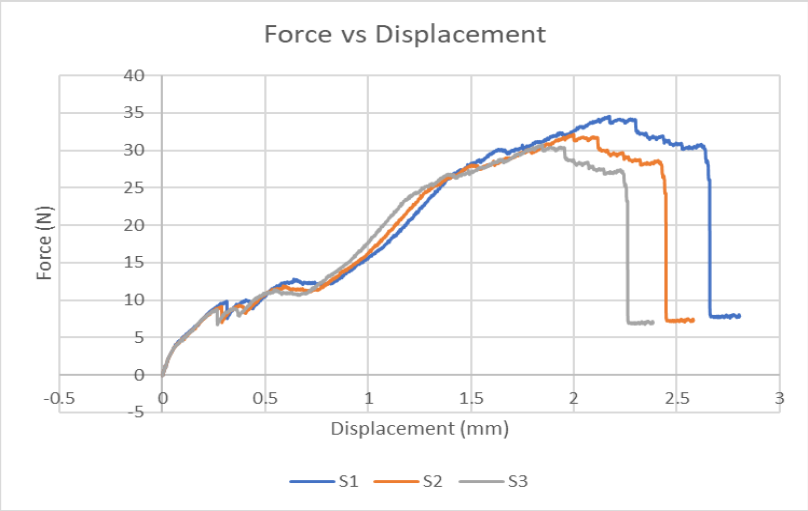

Fig. 5-9 Comparison of peel strength of samples

Using the experimental values, the data is processed and strength and damage properties of Kevlar and Alumina are obtained which are utilized for the Simulation and impact testing of the model made of composite material. Simulation of composite panel subjected to impact were performed for different impact energies. Results were obtained for different dynamic parameters such as impact force, impact energy, absorbed energy, damage dissipation energy etc. Certain variations were observed in results for different range of impact energies. Therefore, the results are discussed in two categories: low impact energy and high impact energy.

5.2 Simulation Results for Low Energy Impact (0-45 J)

5.2.1 Force-Time History

Complete impact process can be described in two phases:

- Pre-rebound phase
- Rebound phase

In the first phase, as the impactor starts to make a contact with the first layer, force at the contact starts to increase progressively along with some peaks and valleys and reaches a maximum. Velocity of impactor reduces to zero and composite panel pushes back the impactor because of elastically stored energy. At the point of maximum force second phase starts and force gradually decreases and returns to zero after the loss of contact between projectile and laminate.

In both the phases, some oscillations are present that are result of local vibrations at the point of measurements as the composite panel continuously oscillated to try to oppose the downward movement of impactor. Due to this continuous resistance, these oscillations in force-time history are observed at the point of measurement. A mismatch is observed between two phases, which is attributed to loss of energy in damage.

Table 5-1 Peak force in all cases of low energy impact

V(ms^{-1})	Peak Force		
	Solid Core	ST-Core	Pure Composite
2	3.3446	3.3383	4.5490
4	6.6251	6.5696	6.9885
6	9.3871	9.3455	11.655
8	13.722	12.379	19.961

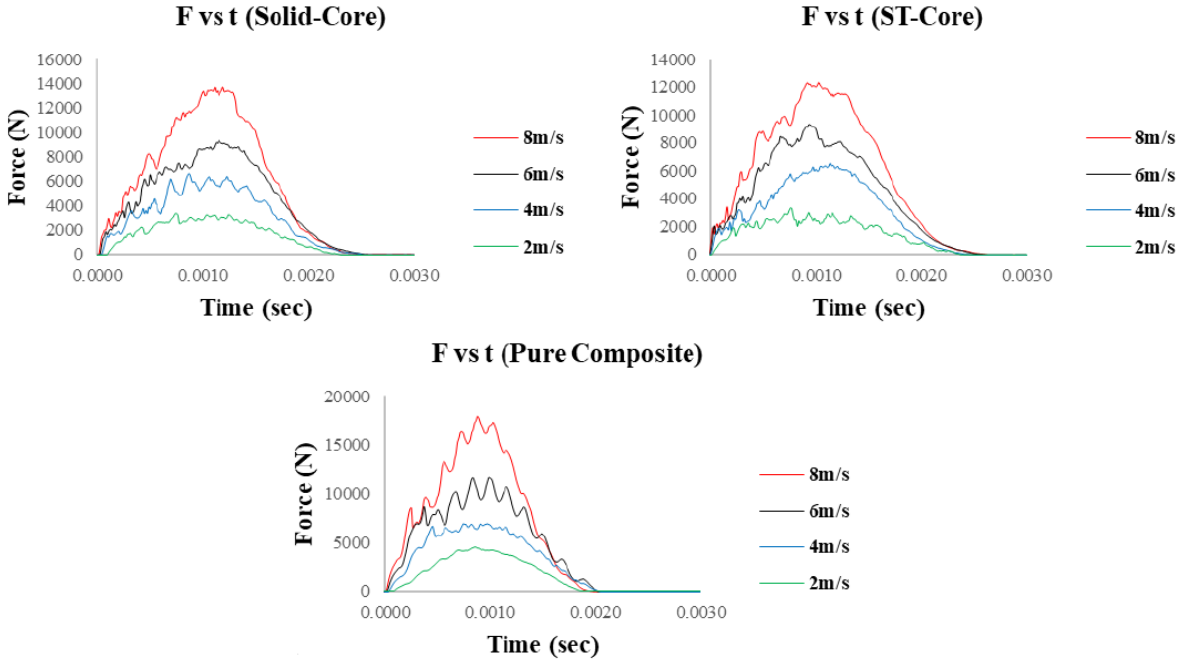

Fig. 5-10 Force-time history of different cases of sandwich core for low energy impact analysis (0-40J)

5.2.2 Force Displacement History

Force displacement history of impactor indicating peak force and displacement of projectile is plotted as shown below. It is indicated that force also returns to zero as impactor detaches from the panel after the rebound phase. Force-displacement history guides about the delamination onset and damage energy dissipation which indicated by the area enclosed by the curve. Similar oscillations are also observed in this case as in force-time history due to local vibrations at local measurement points.

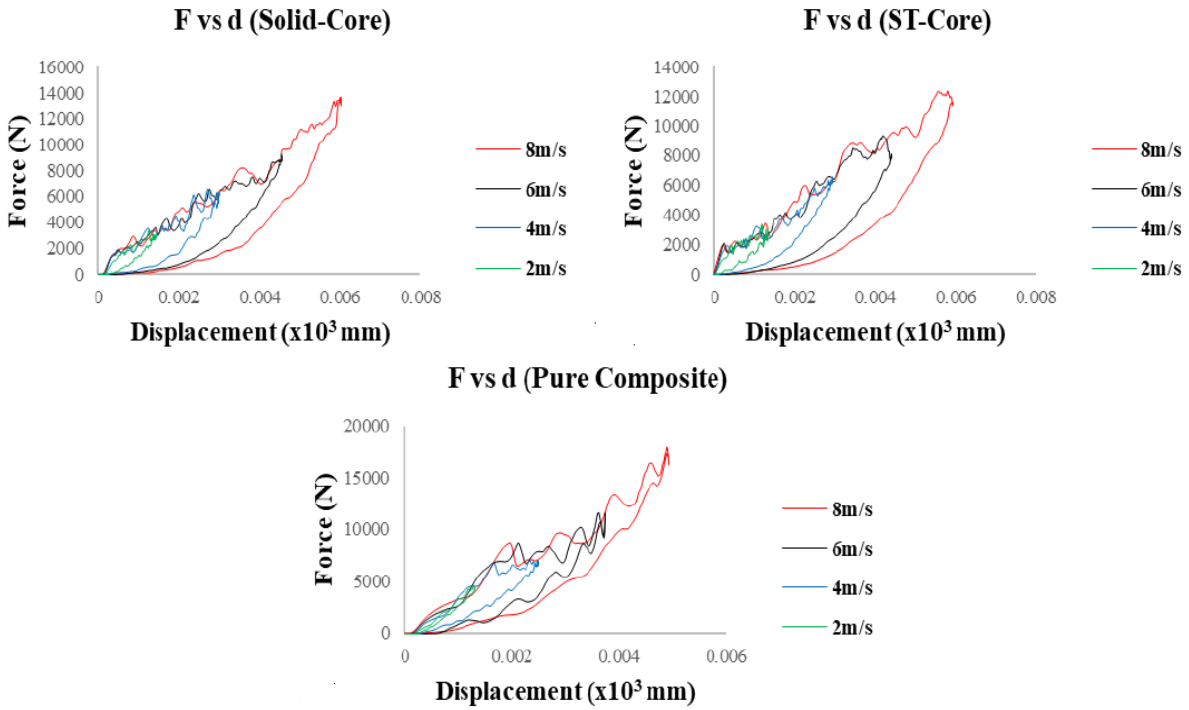

Fig. 5-11 Force-displacement history of impactor for different cases of sandwich core for low energy impact analysis (0-40J)

5.2.3 Energy Absorption

Internal plots give us insight about the contribution of different energies to the system such as elastically absorbed energy or rebound energy, damage dissipation energy, total energy, hourglass contribution, friction dissipation and mass-scaled inertial contribution. Energy vs time plots indicating all the above-mentioned parameters are as follows:

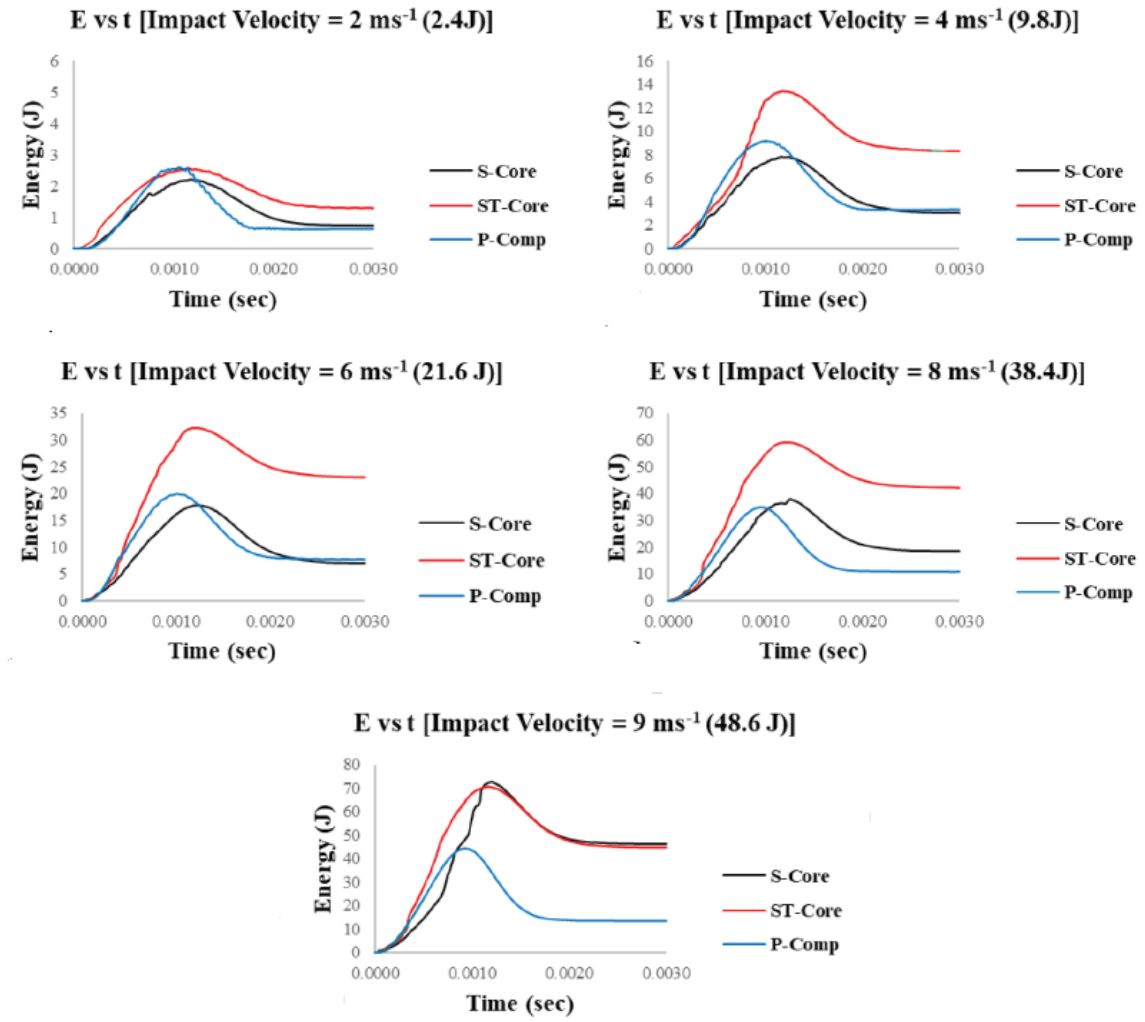

Fig. 5-12 Force-displacement history of impactor for different cases of sandwich core for low energy impact analysis (0-40J)

This is because friction effects are dominant at low energy impacts and despite having very low friction penalties at the cohesive interface, energy plots for two cases mentioned above showed some distorted behaviour. However, above 3J impact energy this problem is avoided as indicated from the plots above. Internal energy increases as the impact phenomenon progresses to reach a maximum and then decreases to stabilize at a certain value. This value is absorbed energy of the system i.e. the energy absorbed by the composite sandwich panel which is the most important of this study.

As we have modelled sandwich core with tiles of different shapes to increase the interface area (cohesive interface area), which is intended to contribute to energy absorption in delamination thus

avoiding fibre fracture to a certain extent. It is clearly indicated from the graphs above that energy absorption increases by increasing the interface area. Square tiles core (ST-Core) model having maximum interface.

Table 5-2 Energy absorbed in all cases for different impact energies.

Impact Energy (J)	**Absorbed Energy (J)**		
	Solid Core	**ST-Core**	**Pure Composite**
2.4 (2 ms^{-1})	0.74	1.31	0.63
9.8 (4 ms^{-1})	3.01	8.33	3.34
21.6 (6 ms^{-1})	6.98	22.99	7.7
38.4 (8 ms^{-1})	18.6	42.2	10.9
48.6 (9 ms^{-1})	46.3	44.9	13.5

However, this phenomenon is observed for a small range of impact energy (0-40J) typically termed as low impact energy. Although the trend remains same as aspect of interface area but as the impact energy increases above 40J solid core shows better energy absorption than all other cases.

However, it is very important to note that placement of sandwich core in between Kevlar layers significantly increases energy absorption as compared to energy absorbed in pure composite structure.

5.2.4 System Energies

Numerical solution of dynamic analysis involves the use some particular techniques to ensure solution convergence, reduction of computational cost and computational time such reduced integration, hourglass control, mass scaling etc.

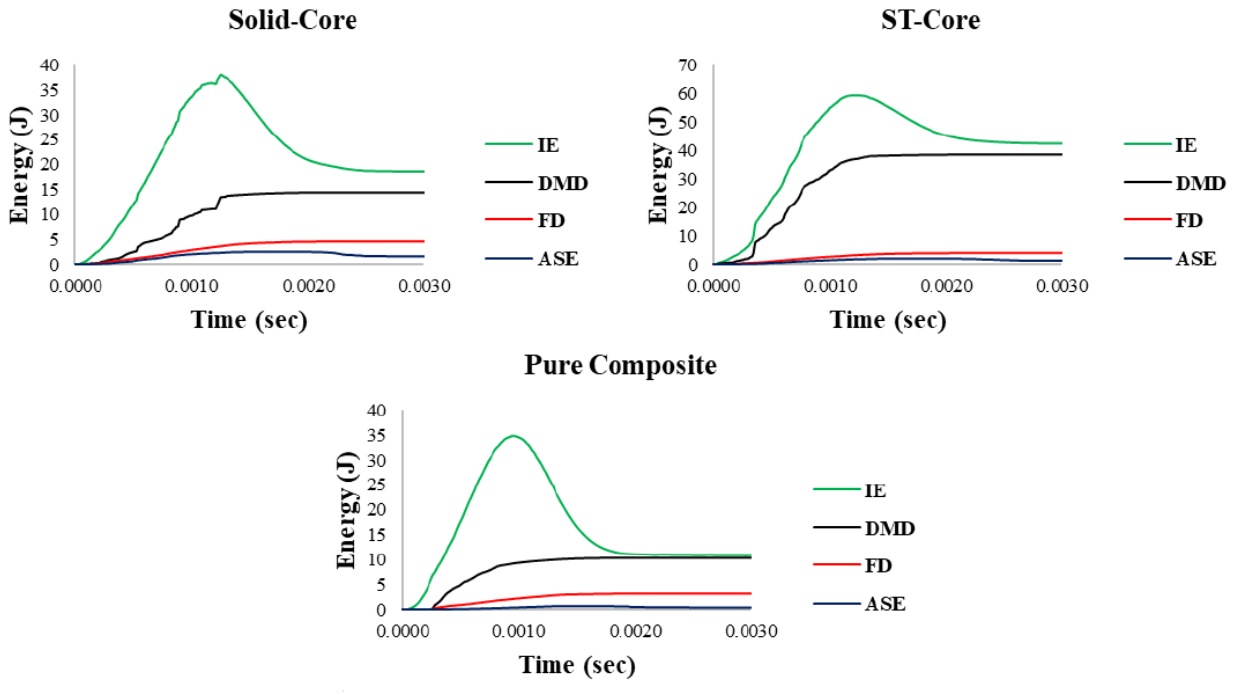

Fig. 5-13 All energy (IE, DMD, FD, ASE) vs time plots for all cases at 8 ms-1 impact velocity [IE: Internal energy; DMD: Damage dissipation energy; FD: Friction dissipation]

However, use of these techniques is very critical and must be carefully controlled to avoid excessive energy contribution as it will change the results significantly. Therefore, it is ensured that the artificial energy contribution due to hourglass control and friction dissipation is less than 10% of internal energy. This can be observed in energy plots shown above.

5.3 Simulation Results for High Energy Impact (>40J)

5.3.1 Force-Time History

Very similar behaviour is observed in force-time history as in the case of low energy impact. Elastic oscillations in pre-rebound phase are reduced significantly, as it is less likely for the panel to cause rebound force application on impactor as traverses downwards. However, force reaches as maximum as velocity becomes zero.

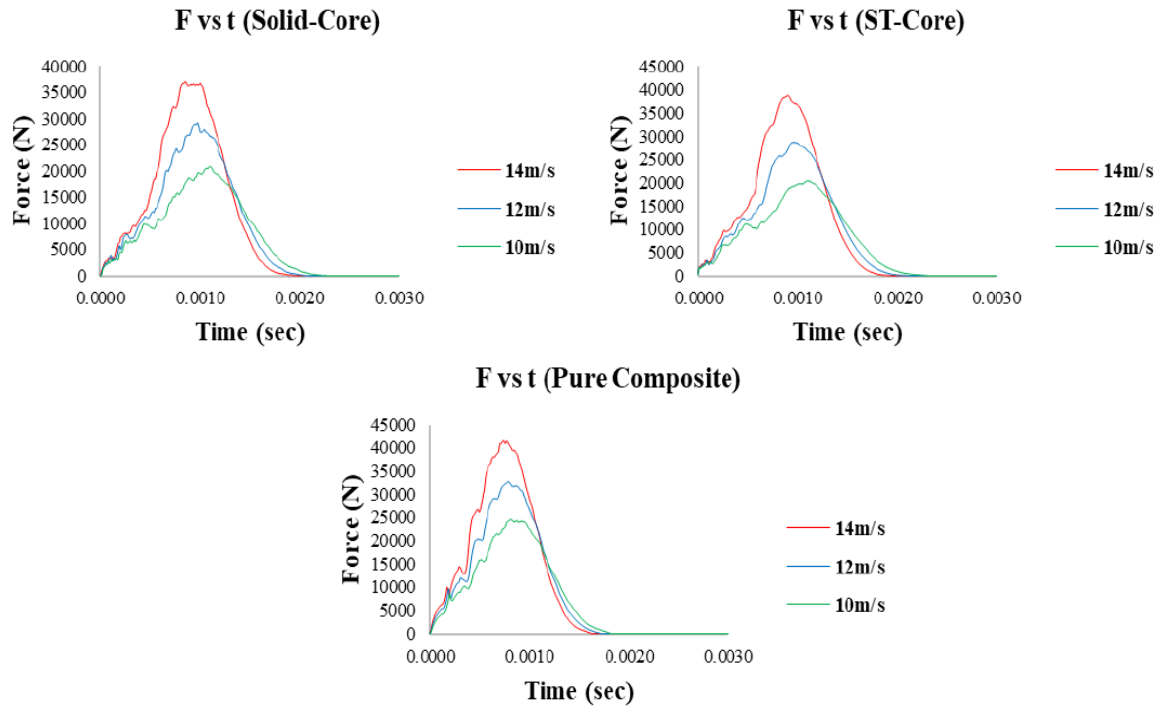

Fig. 5-14 Force-time history of different cases of sandwich core for high energy impact analysis (>40J)

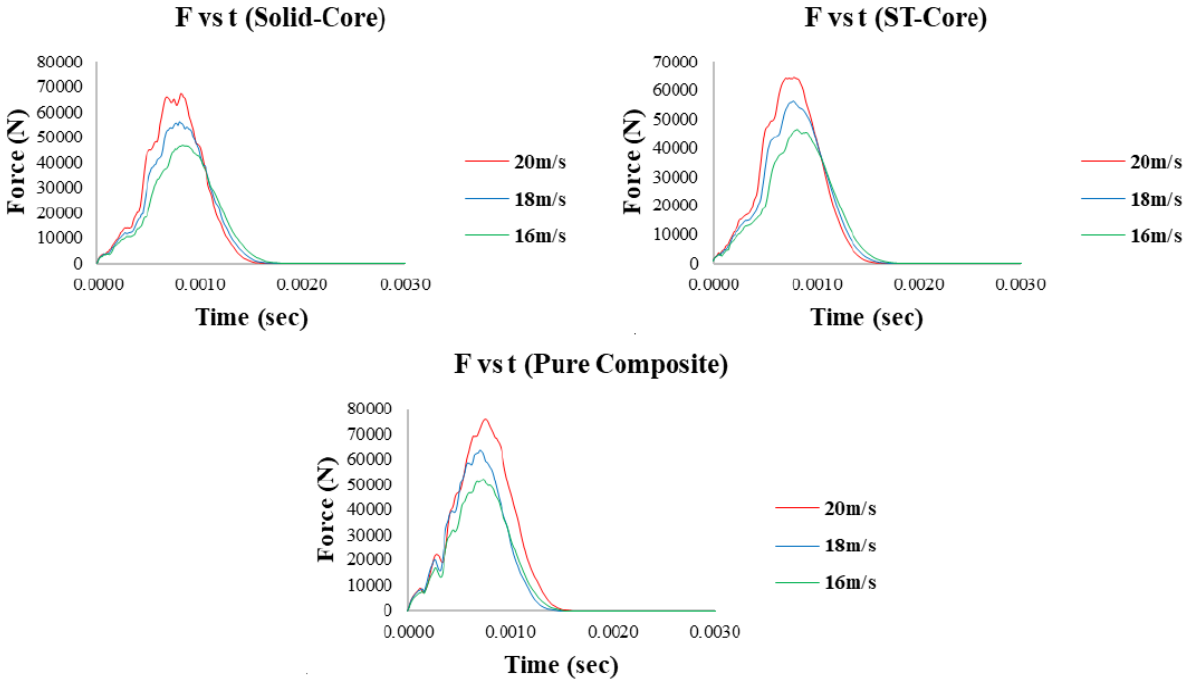

Fig. 5-15 Force-time history of different cases of sandwich core for high energy impact analysis (>40J)

Table 5-3 Peak force in all cases of high-energy impact

V(ms^{-1})	Peak Force (kN)		
	Solid Core	**ST-Core**	**Pure Composite**
10	20.779	20.397	24.675
12	29.189	28.755	32.898
14	37.044	38.578	41.610
16	46.582	46.759	52.215
18	56.401	56.156	63.542
20	67.172	64.595	75.951

5.3.2 Force-Displacement History

Peak force in the impact process and maximum displacement of impactor is indicated in force-displacement history of the phenomenon. Similar to low energy impact, force return to zero after attaining a maximum as the panel and impactor lose contact at the end of rebound phase.

Nevertheless, encapsulated area of curve is relatively small because of low energy absorbing capacity under high rate of loading.

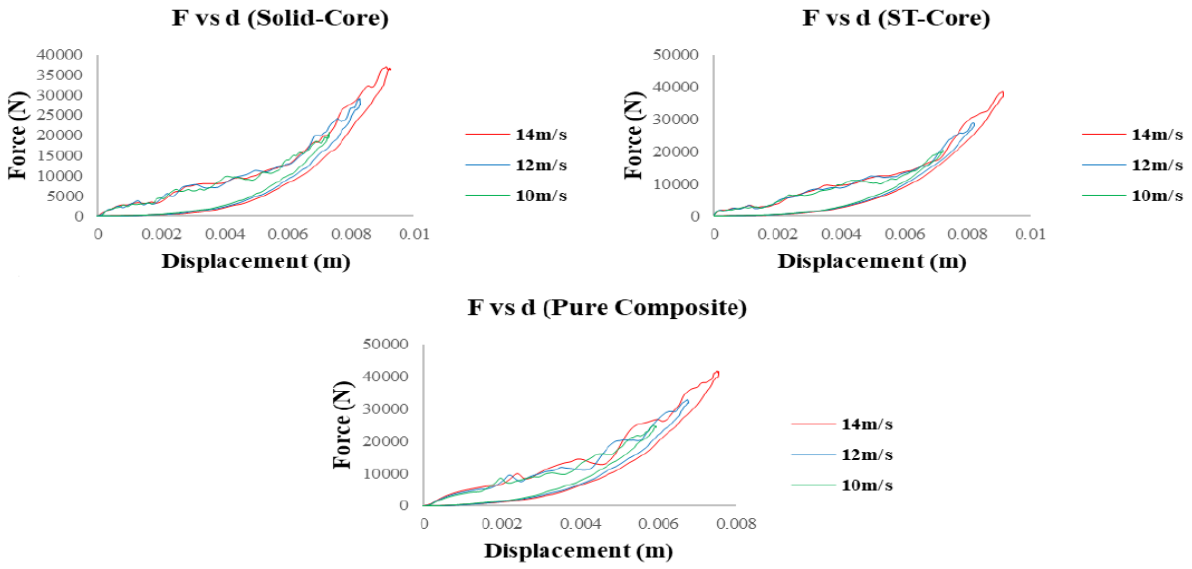

Fig. 5-16 Force-displacement history of impactor for different cases of sandwich core for high energy impact analysis (>40J)

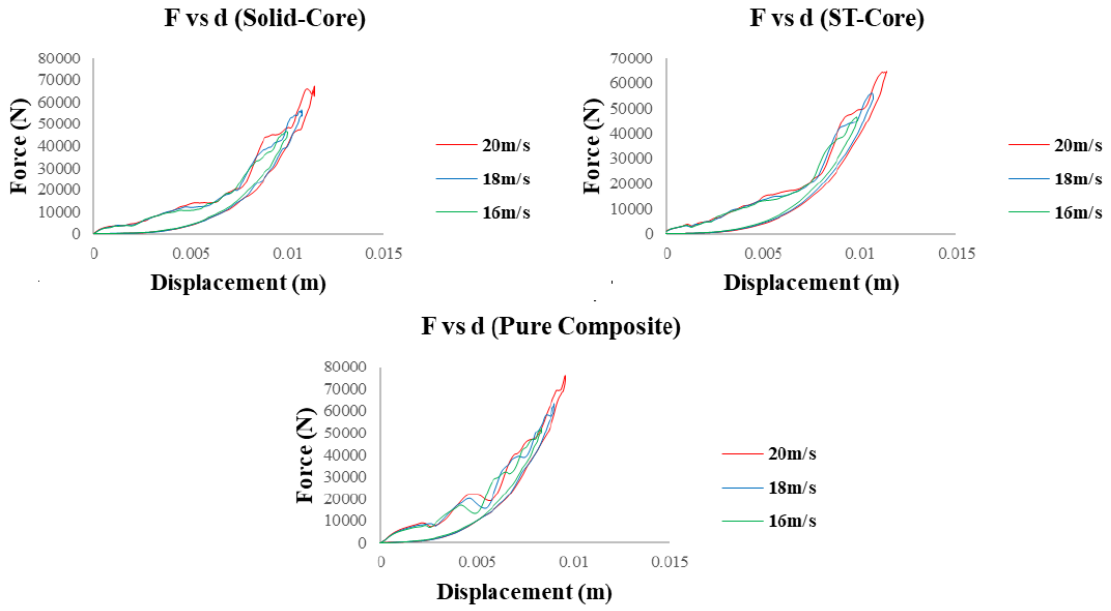

Fig. 5-17 Force-displacement history of impactor for different cases of sandwich core for high energy impact analysis (>40J)

5.3.3 Energy Absorption

As discussed in the previous section, internal energy tells us about the energy absorbed in the system and energy dissipates in damage. Absolute value of dissipated energy is increased as we

increase the impact velocity of the projectile. However, the damage energy dissipation capability suffers a lot as rate of loading rises. As we know that, delamination damage is dominant damage at low rate of loading and fibre cracking is more likely to occur when subjected to high rate of loading. Hence, as the impact energy increases, reaction time decreases for core tiles to be delaminated and get the maximum energy to be dissipated in delamination at the interface of tiles, which is mainly the reason under low energy impact. At increased impact energy, before the delamination at the interface occurs properly core fails at the center in a manner as if it is made of single solid rectangular plate rather than number of small tiles. So, the advantage of using smaller tiles is significantly reduced and simple solid core shows better behaviour. Hence, solid core case has maximum energy dissipation of all the scenarios. However, placement of ceramic sandwich core still has significant advantage as compared to pure composite case.

Table 5-4 Energy absorbed in all cases for different impact energies

Impact Energy (J)	**Absorbed Energy (J)**		
	Solid Core	**ST-Core**	**Pure Composite**
60 (10 ms^{-1})	57.9	46.5	15.6
86.4 (12 ms^{-1})	63.5	50.3	20.3
117.6 (14 ms^{-1})	72.2	55.8	25.9
153.6 (16 ms^{-1})	80.8	64.8	31.40
194.4 (18 ms^{-1})	87.30	74.7	37.60
240 (20 ms^{-1})	95.30	83.5	43.80

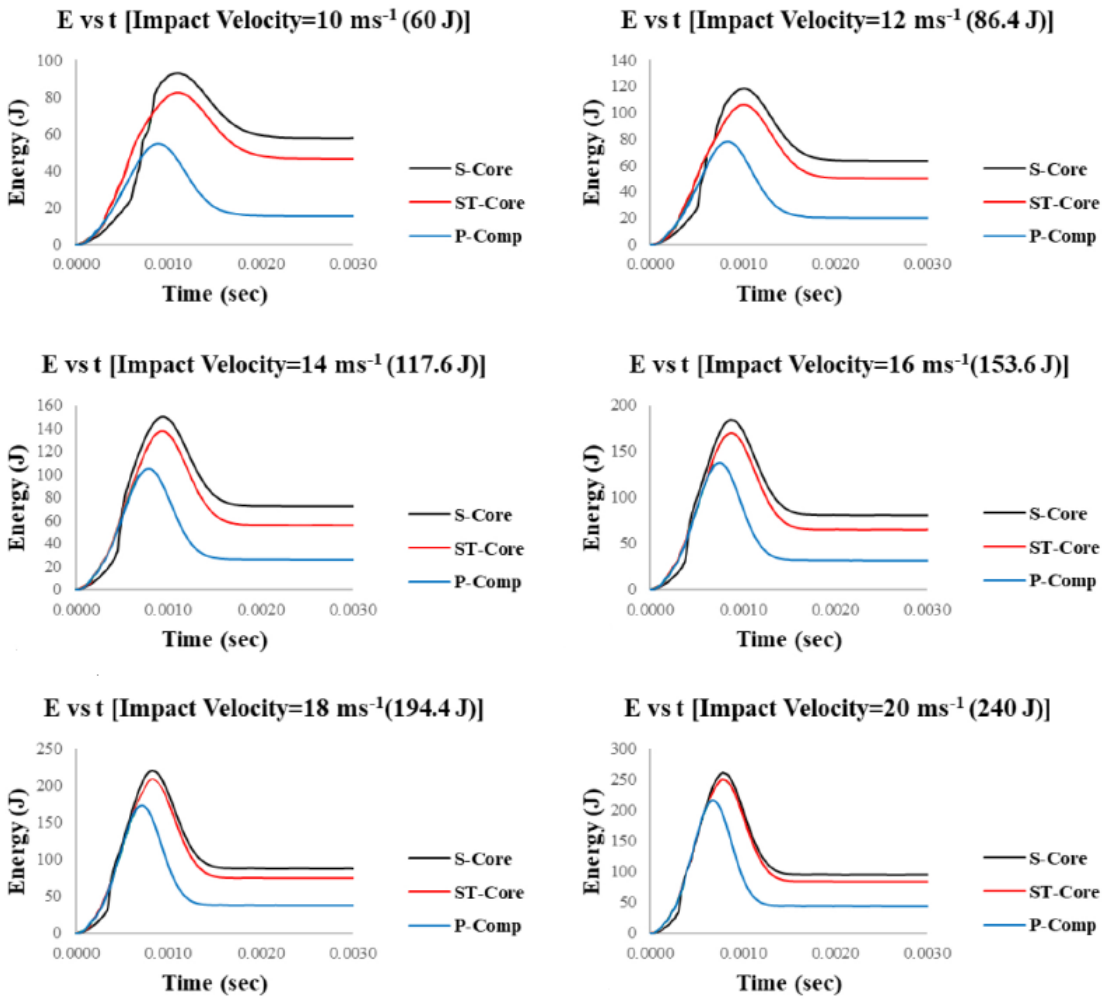

Fig. 5-18 Internal energy vs time for all cases of sandwich core subject to six different impact velocities

5.3.4 Effect of Rate of Loading

It is a fact that rate of loading greatly influences the performance of material, this phenomenon is even more significant in case of composite materials, and attention is paid to this effect as well in the present study. As the rate of loading increases by increasing the impact energy (velocity), material behaviour tends to be more brittle in nature. Strength and stiffness values rise with loading rate and this is clearly indicated from energy vs time plots. The slope of loading phase of energy curve increases as the velocity of projectile increases.

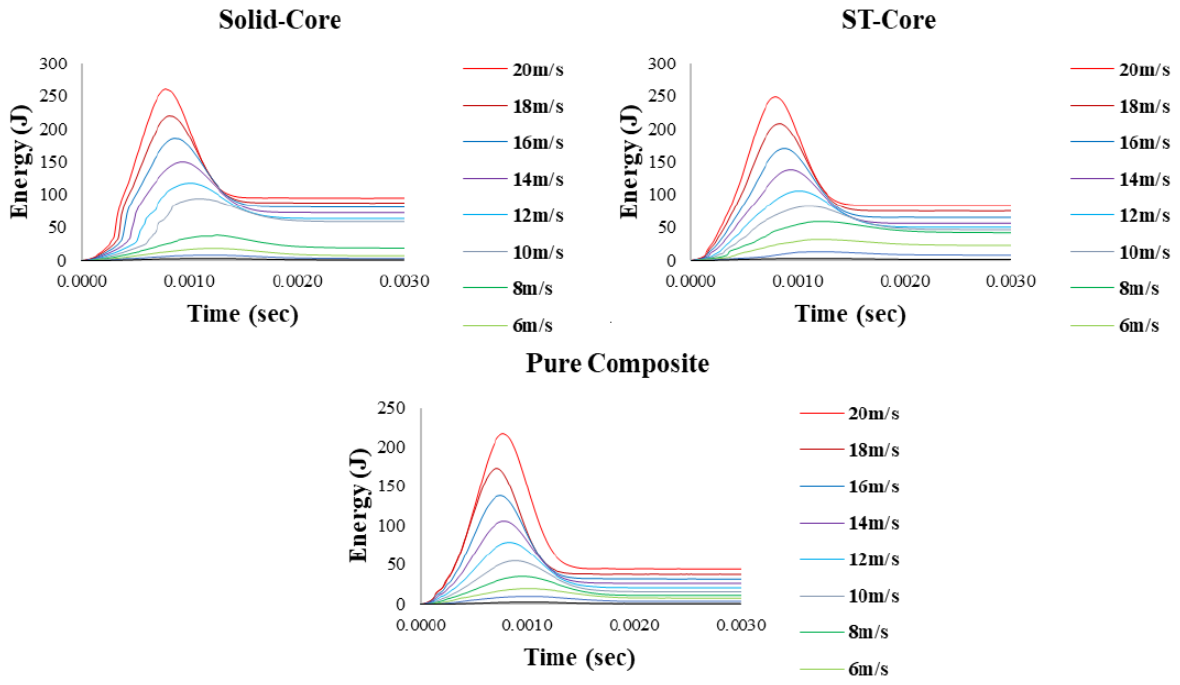

Fig. 5-19 Energy vs Time plots indicating the effect of rate of loading.

5.3.5 Damage

To describe the failure mechanism in composite laminates, careful analysis is performed during simulation to closely observe the different damage pattern. Some specific trends were observed during this process for each of the carious damage modes, which is closely related to the loading conditions, stacking sequence, fibre orientation and placement of ceramic sandwich core. However, similarities are there in the propagation phenomenon of different failure modes with studies that are already performed.

5.3.6 Delamination Damage

Figure shows the distribution of Delamination damage for each layer adopting Hashin failure criteria. Region shown in blue represents undamaged elements while red color indicated the completely damaged elements as the damage variable for the former reaches one as indicated by the values shown in legend. Similar color pattern is followed throughout. Delamination damage is generally expected to initiates at a lower energy level as compared to fibre damage and intralaminar failure modes. Propagation is observed to be along the fibre direction of lower lamina

at the interface which is in correlation with Liu et al. Through-thickness interplay shear stresses govern the delamination damage propagation. In impact loading conditions, these stresses are maximum at the lower ply of the two at the interface due to which delamination failure is mainly follows the fibre direction of lower lamina. In context to shape, delamination nucleates from the center at the point of impact and moves readily outward parallel to fibre orientation which is consistent with Sanan et al. Delamination area increases with increasing impact energy and becomes unstable at very high impact energies.

5.3.7 Matrix Tensile Damage

Matrix tensile damage first initiates on the back surface of each layer and then propagates to impact surface (top surface). Damage shape indicates that failure start to develop at the center (impact region) moving along the fibre direction (radially outward) quickly and phenomenon is much slow in fibre perpendicular direction. It is observed that predicted matrix tensile damage area increases as we move further away from the impact side.

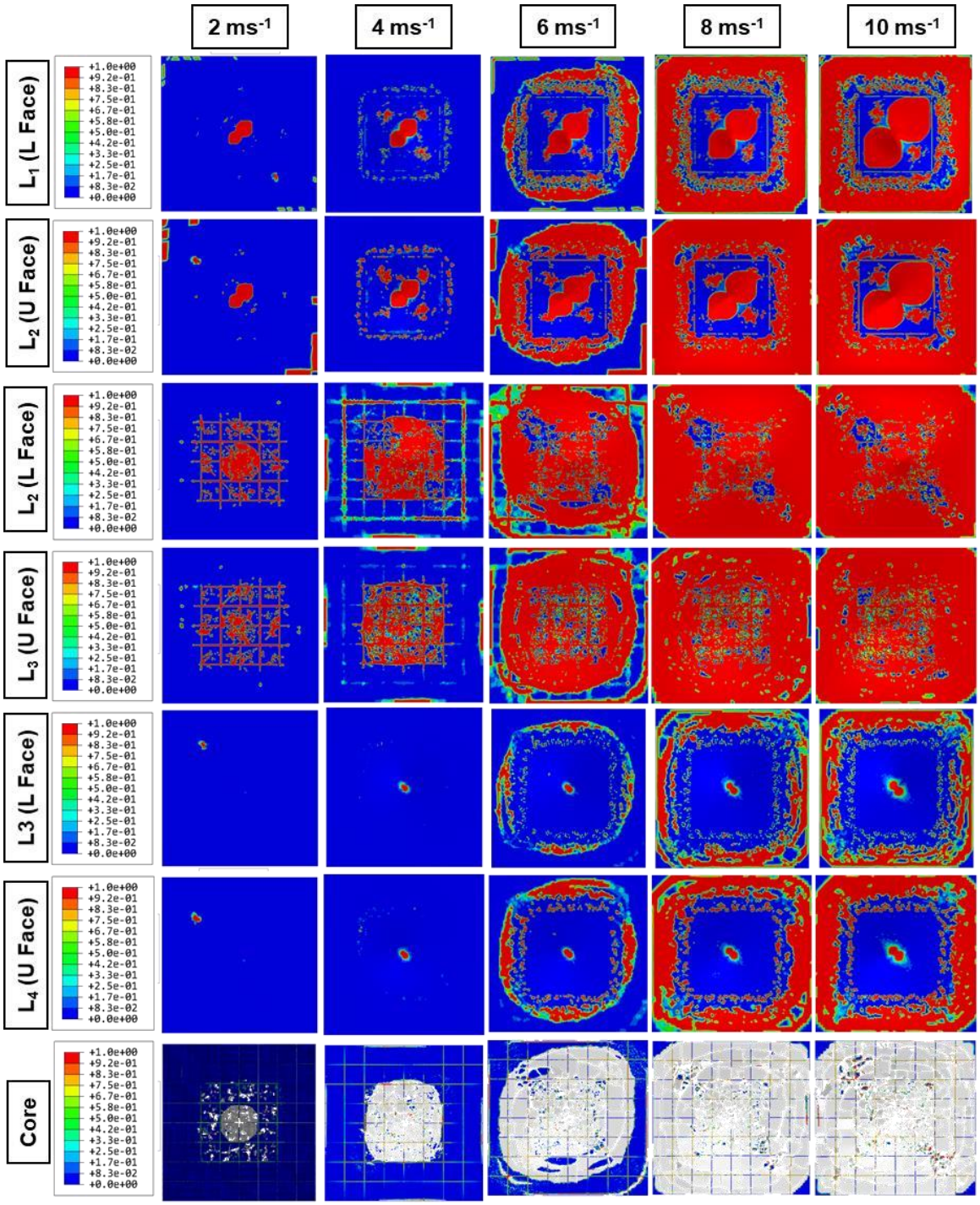

Fig. 5-20 Delamination Damage at the interface of different layer for increasing velocities from left to right (2-10 ms^{-1}) and Core damage pattern for the case of Square Tile Core (U Face = Upper face, L Face = Lower face)

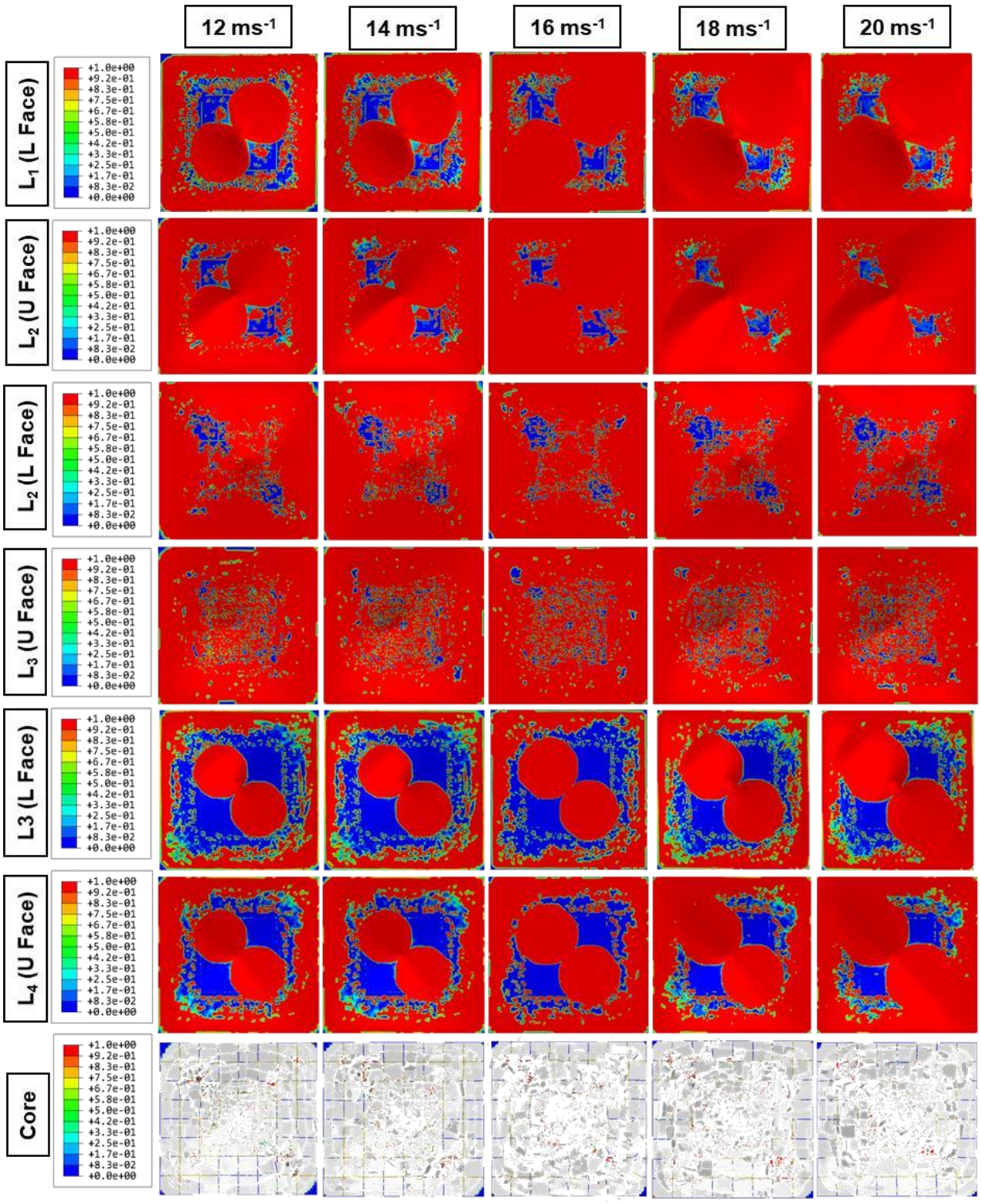

Fig. 5-21 Delamination Damage at the interface of different layer for increasing velocities from left to right (12-20 ms^{-1}) and Core damage pattern for the case of Square Tile Core (U Face = Upper face; L Face = Lower face)

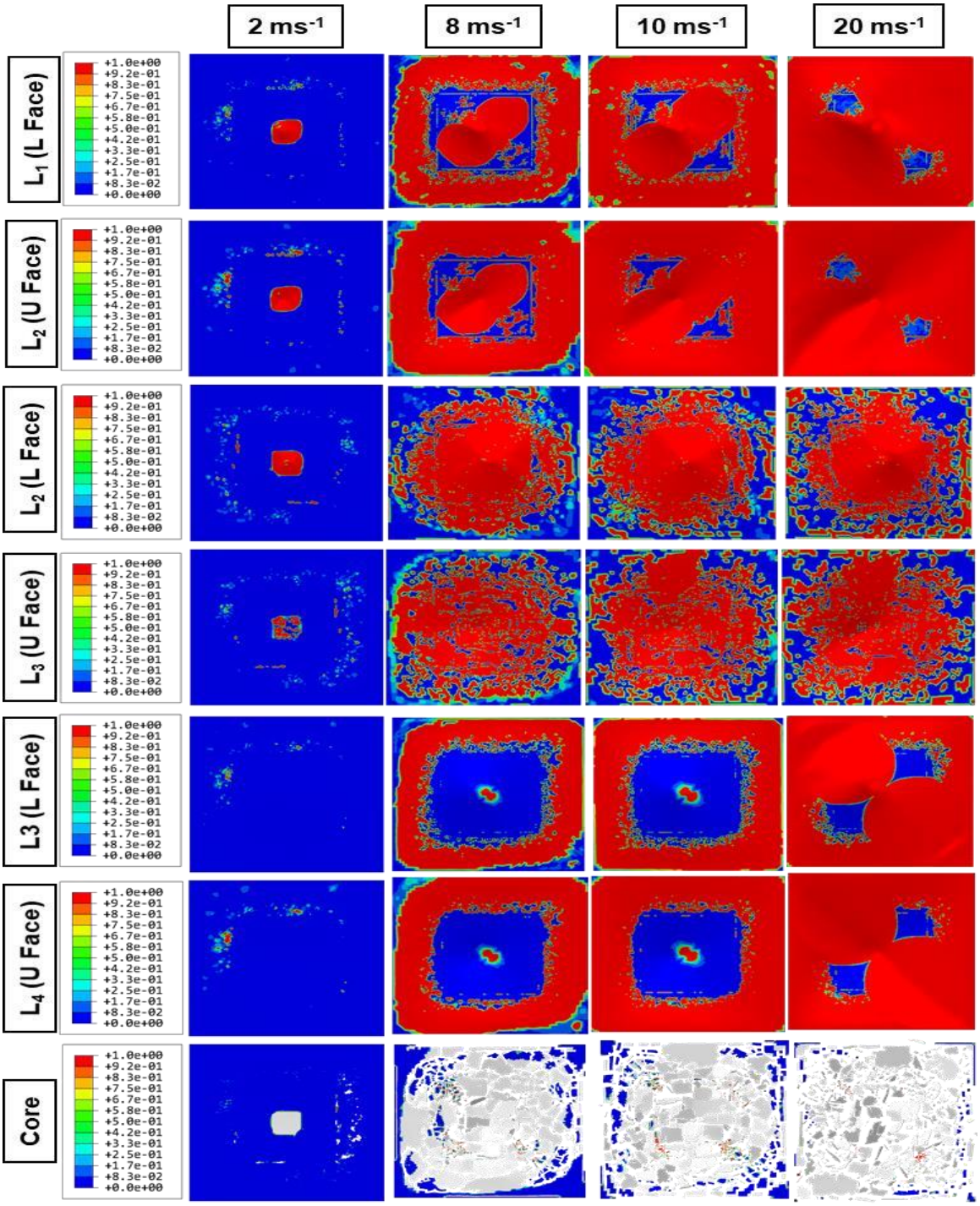

Fig. 5-22 Delamination Damage at the interface of different layer for increasing velocities from left to right (2-20 ms^{-1}) and Core damage pattern for the case of Solid Core (U Face = Upper face; L Face = Lower face)

5.3.8 Fibre Damage

In impact events, both fibre and matrix failure mode appear with fibre failure followed by a matrix failure because of its higher strength. At lower impact energy, there are very few elements with fibre damage in each of laminate as indicated in figure below and is not a serious damage state. Hence, it is concluded that fibre damage tends to begin at comparatively high-energy impact loads. Impact region of projectile and impact surface is the mainly the center for fibre compressive damage because of low compressive strength and high stresses in that particular region. This result in oscillation in force-time history and a sudden drop in force because of significantly lowered load-bearing capacity in out of plane direction. Whereas, fibre tensile damage start at the lower surface in a ply because of high tensile stresses at the lower surface and propagates towards upper surface. It is also due to the fact that fibres a very low transverse tensile strength resulting in very small load bearing capability.

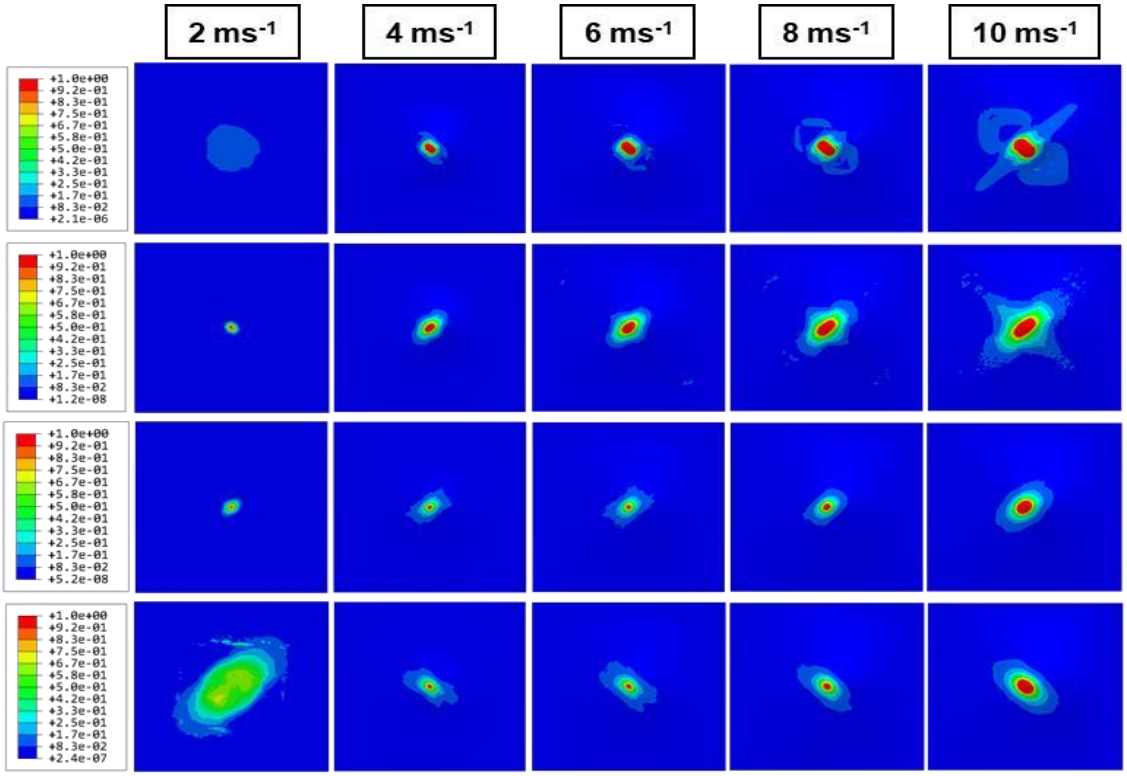

Fig. 5-23 Fibre tensile damage at the bottom face of each layer in case of Square Tiles Core (ST-Core) for increasing velocity of (2-10 ms^{-1})

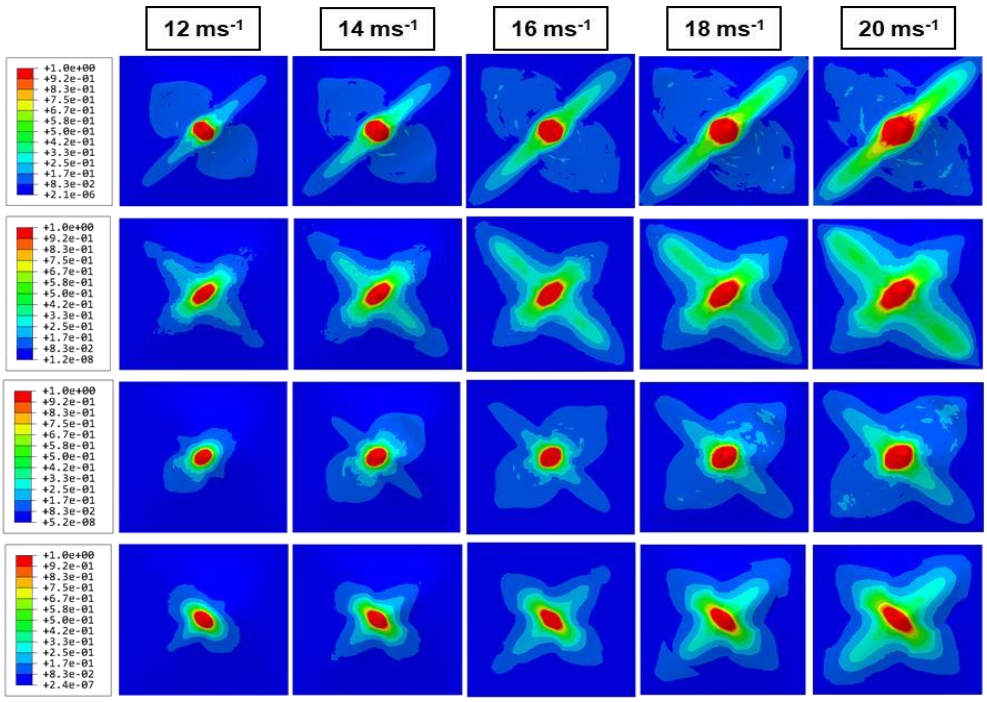

Fig. 5-24 Fibre tensile damage at the bottom face of each layer in case of Square Tiles Core (ST-Core) for increasing velocity of (12-20 ms^{-1})

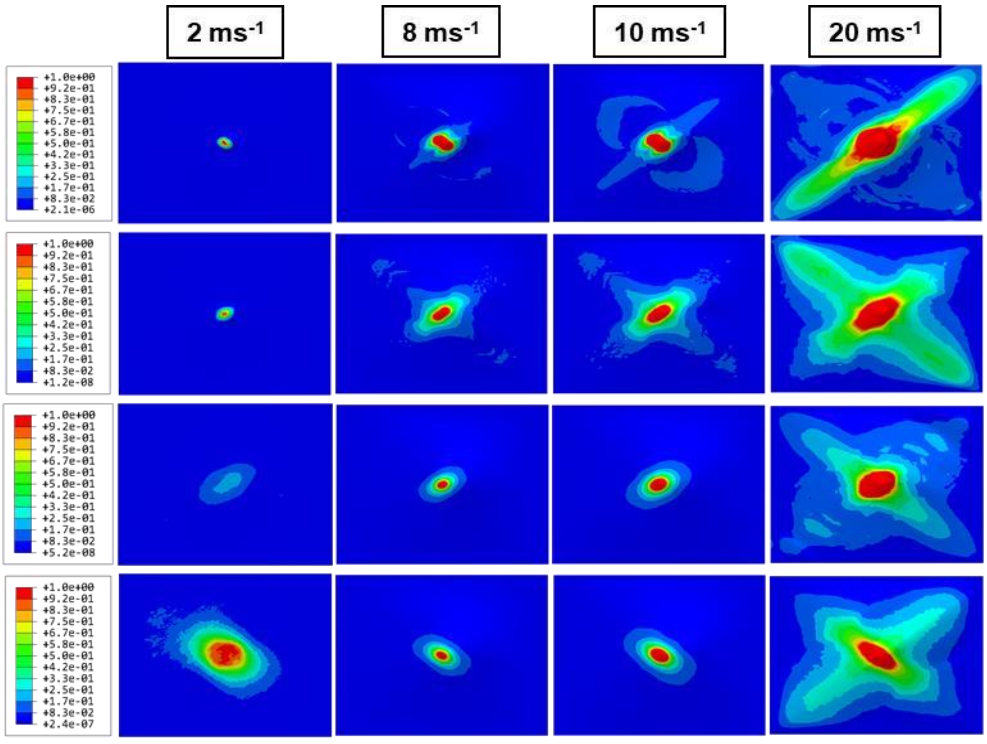

Fig. 5-25 Fibre tensile damage at the bottom face of eac`h layer in case of Solid Core (SC-Core) for increasing velocity of (2-20 ms^{-1})

5.3.9 Damage Accumulation Process

Matrix tensile damage is quick in nature than matrix damage in compression. The sole reason behind this is more significant tensile deformation under impact loads. As soon as matrix tensile damage start to initiate transverse load carrying capacity is significantly drops and as a result, matrix tensile damage variable rises from 0 to 1. Compression damage initiates at the center and propagates in a butterfly shape. Typical damage energy accumulation curve is shown below along with force. As the force starts to rise, damage begin to develop slowly due to initial matrix cracking and then increases suddenly due delamination initiation. Dissipation goes on increasing with force until it reaches a maximum. After the peak, force drop occurs due to rebounding of impactor and hence, damage dissipation energy stabilizes to a certain value.

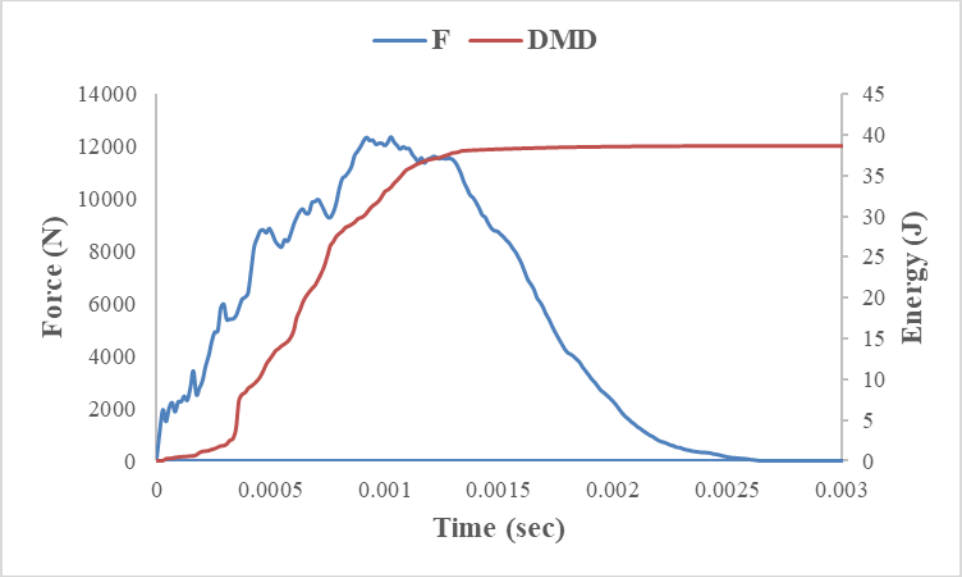

Fig. 5-26 Damage dissipation energy along with force-time history

Chapter 6

6. Conclusions & Recommendation

6.1 Conclusion

A mathematical model of composite structure under impact load for the determination of impact energy, absorbed energy and rebound energy is proposed based fracture energy approach. Hertz's approach is used to analytically predict force-time history of the projectile subjected to impact with composite panel. Core is modelled using solid core and square tiles to increase the interface area, which comes out to be maximum in case of square tiles. ABAQUS explicit dynamics is used for the numerical solution of the impact problem. Cohesive zone modelling (CZM) is used to model the interface delamination between different plies and between the interfaces of different tiles of the core. Hashin damage mechanism is used to model the matrix and fibre damage modes. Mesh convergence study is performed for different number of elements keeping in view the energy absorption and damage patterns.

It is observed that energy absorption increases by increasing interface area core under low energy impact events typically in the range of 0-40J. Square tiles core has the maximum energy absorption. 60% increase in energy absorption is observed due to placement of ceramic core at low energy impact. Whereas, increasing the impact energy above 40J, simple solid core shows maximum energy absorption as compared to other cases. However, trend for interface area remains same with gradually decreasing difference in absorbed energy. And a significant increase of 40-60% in energy absorption is observed for inclusion of ceramic core. Having said that, placement of ceramic sandwich core significantly increases energy absorption as compared to pure composite scenario at both low and high-energy impact events.

Talking about damage, both fibre and matrix failure modes occur in impact events. However, matrix damage is followed by fibre damage due to its comparatively low strength. Usually, all the damage modes initiate at the center with gradual outward propagation, dominant along the fibre direction, in each layer. Moreover, fibre tensile damage is dominant at the lower face of the laminate and compression damage is significant on impact side. Similarly, delamination damage propagation follows the fibre orientation of lower ply of the two at the interface.

6.2 Future Recommendation

Some recommendation for further research to extend the present work are mentioned as following:

- The present study can be extended for optimization of tile size according to possible preparation of samples.
- Different criteria (Puck criteria for matrix compression and Tsai-Hill criteria) can be employed to further investigate the variation of energy absorption in different damage modes.
- Experiments be performed for better analysis of results especially in case of friction dissipation.
- Tile shapes and size can be optimized based on availability, cost and ease of preparation.
- Visco-elasticity and visco-plasticity can be incorporated to consider material property variation with rate of loading.
- The model can be extended to determine the contribution of each damage mode in energy absorption in VUMAT.

References

[1] Z. Hashin and A. Rotem, “A Fatigue Failure Criterion for Fiber Reinforced Materials,” *J. Compos. Mater.*, vol. 7, no. 4, pp. 448–464, 1973, doi: 10.1177/002199837300700404.

[2] S. Nak-Ho and N. P. Suh, “Effect of fiber orientation on friction and wear of fiber reinforced polymeric composites,” *Wear*, vol. 53, no. 1, pp. 129–141, 1979, doi: 10.1016/0043-1648(79)90224-2.

[3] M. Kenane and M. L. Benzeggagh, “Mixed-mode delamination fracture toughness of unidirectional glass/epoxy composites under fatigue loading,” *Compos. Sci. Technol.*, vol. 57, no. 5, pp. 597–605, 1997, doi: 10.1016/S0266-3538(97)00021-3.

[4] Z. Hashin, “Failure criteria for unidirectional fiber composites,” *J. Appl. Mech. Trans. ASME*, vol. 47, no. 2, pp. 329–334, 1980, doi: 10.1115/1.3153664.

[5] J. Sch??n, “Coefficient of friction of composite delamination surfaces,” *Wear*, vol. 237, no. 1, pp. 77–89, 2000.

[6] S. Chattopadhyay and R. Saxena, “Combined effects of shear deformation and permanent indentation on the impact response of elastic plates,” *Int. J. Solids Struct.*, vol. 27, no. 13, pp. 1739–1745, 1991, doi: 10.1016/0020-7683(91)90072-N.

[7] ABAQUS Inc, “Analysis Theory Manual version Abaqus 6.11,” vol. I.

[8] C. G. Dávila, P. P. Camanho, and A. Turon, “Cohesive elements for shells,” *Nasa/Tp-2007-214869, L-19341*, no. April 2007, p. 27, 2007.

[9] K. N. Shivakumar, W. Elber, and W. Illg, “Prediction of impact force and duration due to low-velocity impact on circular composite laminates,” *J. Appl. Mech. Trans. ASME*, vol. 52, no. 3, pp. 674–680, 1985, doi: 10.1115/1.3169120.

[10] A. Tasdemirci, A. Kara, A. K. Turan, G. Tunusoglu, M. Guden, and I. W. Hall, “Experimental and numerical investigation of high strain rate mechanical behavior of a [0/45/90/-45] quadriaxial e-glass/polyester composite,” *Procedia Eng.*, vol. 10, pp. 3068–3073, 2011, doi: 10.1016/j.proeng.2011.04.508.

[11] M. M. Shokrieh and M. O. Jamal, “Development of a strain-rate dependent progressive damage model for crash analysis of composite laminates,” no. December 2013, pp. 1263–1269, 2009, doi: 10.1051/dymat/2009178.

[12] A. Mostafa, K. Shankar, and E. V. Morozov, “In-plane shear behaviour of composite sandwich panel incorporated with shear keys methodology at different orientations: Finite element study,” *J. Compos. Mater.*, vol. 48, no. 24, pp. 2945–2959, 2014, doi: 10.1177/0021998313503588.

[13] C. L. Tsai and I. M. Daniel, “Determination of in-plane and out-of-plane shear moduli of composite materials,” *Exp. Mech.*, vol. 30, no. 3, pp. 295–299, 1990, doi: 10.1007/BF02322825.

[14] N. Manap, A. Jumahat, and N. Sapiai, “Effect of fibre treatment on longitudinal and transverse tensile properties of unidirectional kenaf composite,” *J. Teknol.*, vol. 76, no. 11, pp. 87–95, 2015, doi: 10.11113/jt.v76.5918.

[15] M. Ravi Sankar, M. Lava Kumar, and S. Haribabu, “Tensile Behaviour of BBJS

Composite Materials," *Int. J. Eng. Trends Technol.*, vol. 17, no. 3, pp. 147–150, 2014, doi: 10.14445/22315381/ijett-v17p230.

[16] T. Nadabe and N. Takeda, "Numerical simulation and theoretical modeling of longitudinal compressive failure in fiber reinforced composite materials," *Int. Conf. Logist. Eng. Manag. Comput. Sci. LEMCS 2014*, no. May, pp. 908–917, 2014, doi: 10.2991/lemcs-15.2015.56.

[17] R. Thompson, "Compressive Strength of Continuous Fiber Unidirectional Composites," 2012.

[18] N. K. Naik and R. S. Kumar, "Compressive strength of unidirectional composites: Evaluation and comparison of prediction models," *Compos. Struct.*, vol. 46, no. 3, pp. 299–308, 1999, doi: 10.1016/S0263-8223(99)00098-7.

[19] F. Alkhatib, E. Mahdi, and A. Dean, "Design and evaluation of hybrid composite plates for ballistic protection: Experimental and numerical investigations," *Polymers (Basel).*, vol. 13, no. 9, pp. 1–15, 2021, doi: 10.3390/polym13091450.

[20] T. K. Ćwik, L. Iannucci, P. Curtis, and D. Pope, "Design and Ballistic Performance of Hybrid Composite Laminates," *Appl. Compos. Mater.*, vol. 24, no. 3, pp. 717–733, 2017, doi: 10.1007/s10443-016-9536-x.